



“Neutron and Rheology”

Mitsuhiro Shibayama,
ISSP, U. Tokyo

Part 1. Structural Analyses of Polymers by
Small Angle Neutron Scattering

Part 2. Contrast Variation SANS
- The basics and applications -

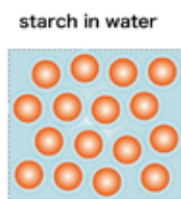
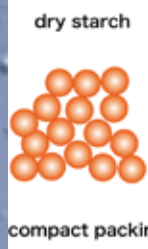
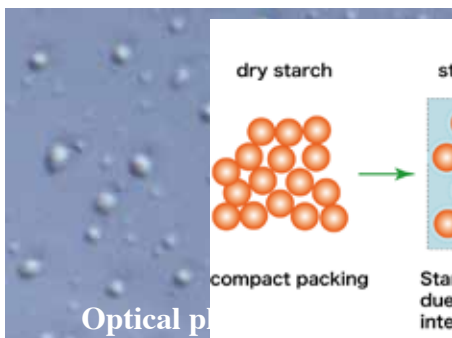
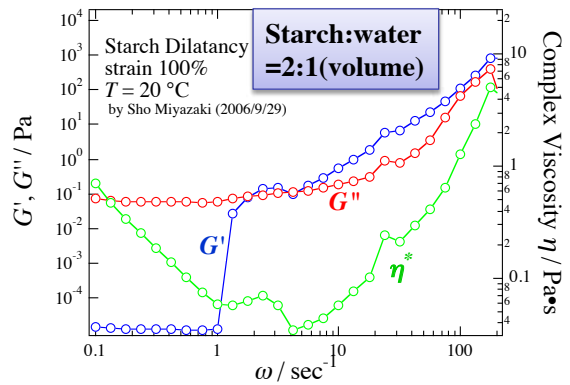
Part 3. Rheo-SANS Studies on Structure Evolution
in Polymer-particle Aqueous Solutions
- shear thickening -



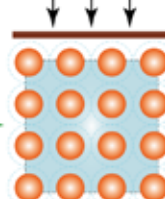
Dilatancy



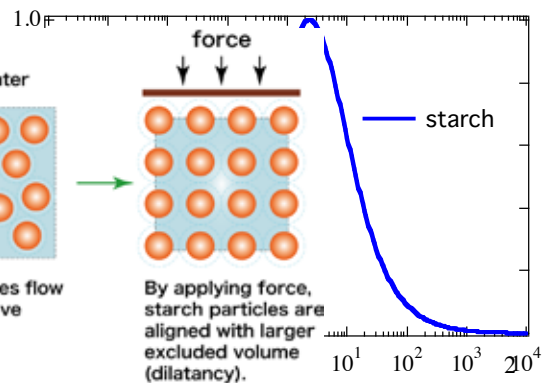
Concentrated
starch dispersion in water



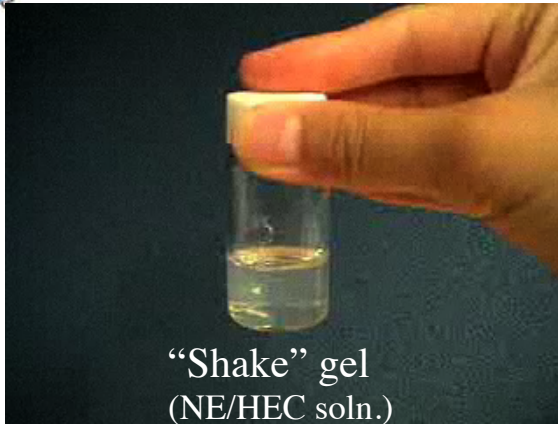
Starch particles flow
due to repulsive
interaction.



By applying force,
starch particles are
aligned with larger
excluded volume
(dilatancy).



shear thickening of starch suspension



Laponite (clay)-PEO

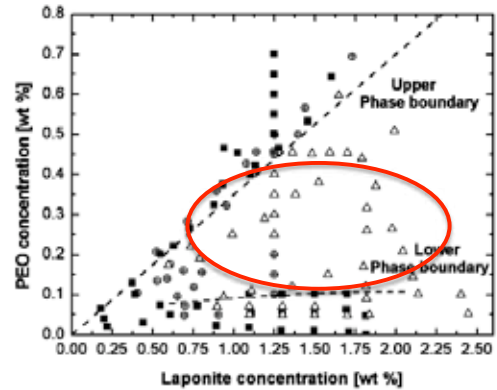
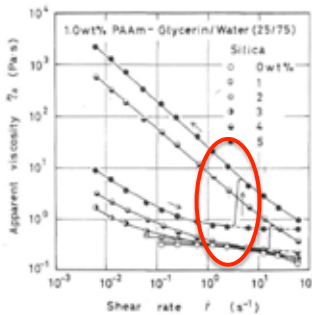


Fig. 1. Phase behavior of laponite-PEO 'shake-gels', formed by vigorous shaking. The open triangles represent mixtures that form shake-gels upon application of shear; the circles represent mixtures that shear-thicken and show an increase in viscosity but do not gel; and the solid squares represent mixtures that do not gel even when subjected to large shear. The molecular weight of PEO used is $M_w = 300\,000 \text{ g mol}^{-1}$, with a radius of gyration $R_g = 32 \text{ nm}$.



Silica-PA

Silica suspensions in polyacrylamide solutions

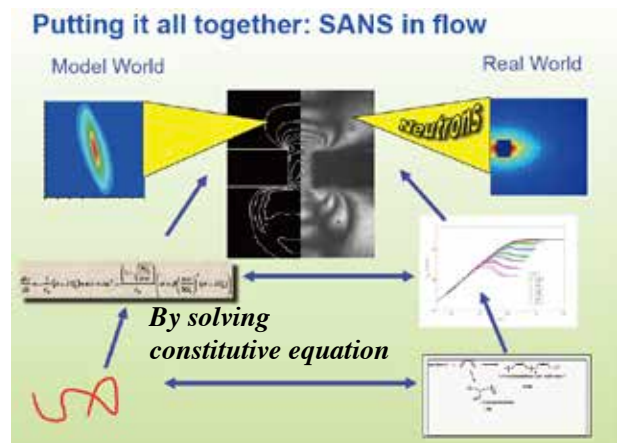
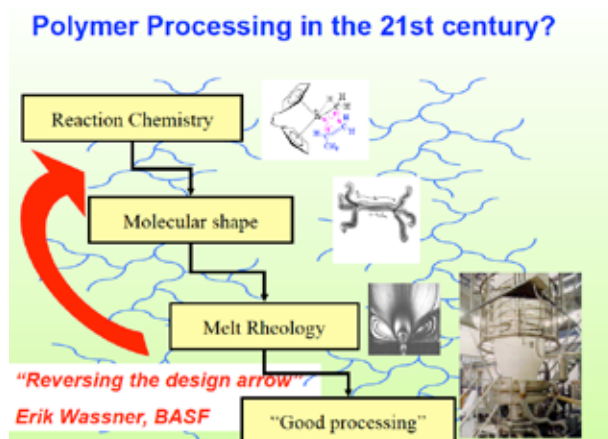
Y. Otsubo, K. Umeya
J.Rheology, 1984, 28, 95-108.

Fig. 7. Shear rate dependence of apparent viscosity for 1.0 wt % PAAm solution in glycerin/water mixture with 25/75 mixing ratio and the suspensions at different particle concentrations.

Shear-induced gelation of laponite-PEO mixtures
J. Zebrowski, D. A. Weitz et al.
Colloid Surface and Interface, 213, 2003, 189.

Advances in Rheo-SANS: The structural rheology of long polymer chain branched polymers

Measuring and modelling of macromolecules in flow



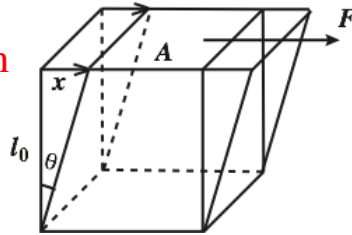


Shear deformation and response

= variety of rheological behavior of polymeric systems =

Rheology; science to understand the relationship between deformation and its response

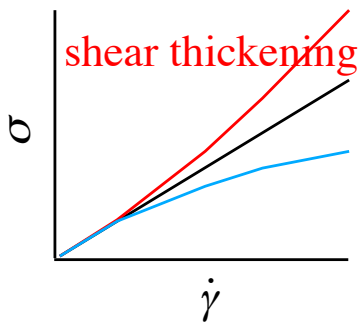
Shear deformation
shear



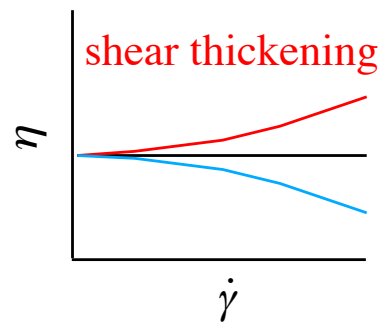
Stress: $\sigma = F / A_0$

Shear strain: $\gamma = l_0 / x = \tan\theta$

Shear rate: $\dot{\gamma} = \frac{d\gamma}{dt}$



$\sigma / \dot{\gamma} = \eta$



e.g.) Shear thinning ; ketchup, mayonnaise, cosmetics, paints
Shear thickening ; starch, sand of seashore



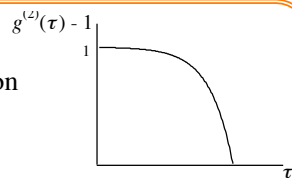
Experimental

ALV-5000

dynamics

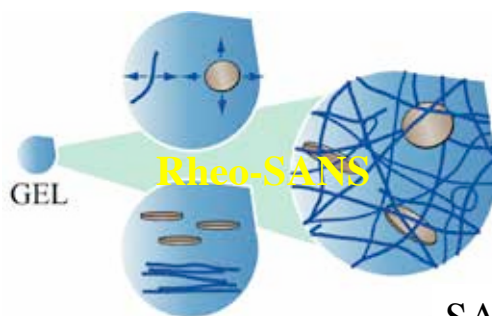
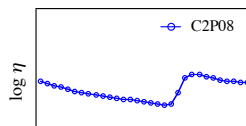
diffusion
Translation/local motion

DLS



properties

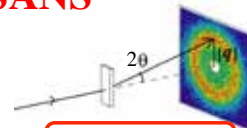
viscometry



structure

Intermolecular
interaction

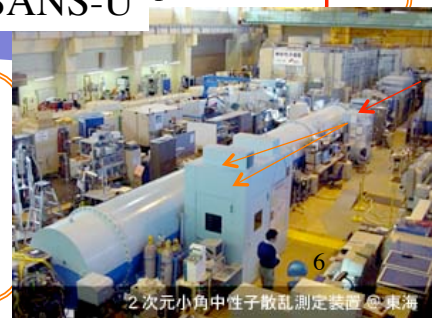
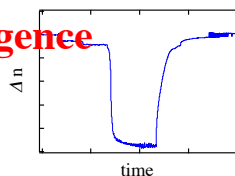
SANS



SANS-U $q = 4\pi/\lambda \sin\theta$

small
orientation

birefringence



Rheo-SANS



SANS-U, ISSP, Univ. Tokyo

Wavelength: 7 Å

SDD: 2, 4, 8 m, 12 m

Q range: 0.002 - 0.1 Å⁻¹

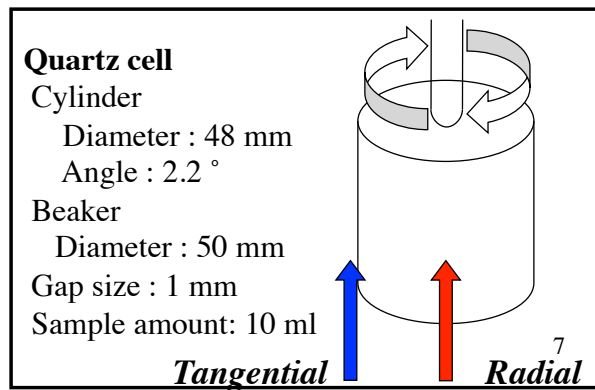
Okabe et al., J. Appl. Cryst., 2005, 38, 1035.

Iwase et al., J. Appl. Cryst., 2011, 44, 558.

MCR 501 (Anton Paar)

Torque : 0.1 μNm - 230 mNm

Torque resolution : 0.001 μNm



Tree topics

Part I: NE/HEC Shake gel

Part II: Shear thickening of Clay/PEO

Part III: Phantom chains of CTAB/salt

Tree topics

Part I: NE/HEC Shake gel

Part II: Shear thickening of Clay/PEO

Part III: Phantom chains of CTAB/salt

9

Self-standing nano-emulsion

Kawada, et al., Langmuir, 2010, 26, 2430.



self-standing
Nano-emulsion

About 25% oil droplet

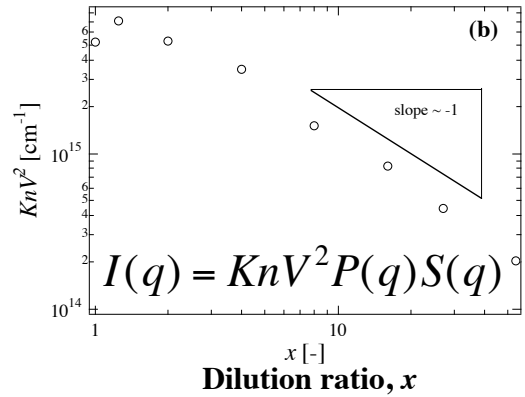
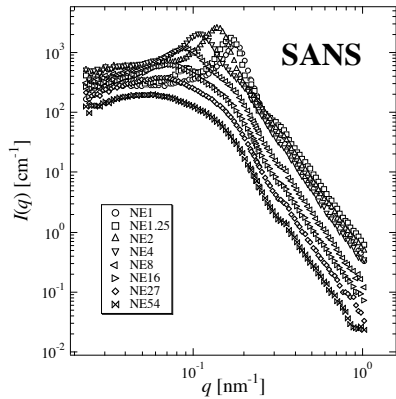
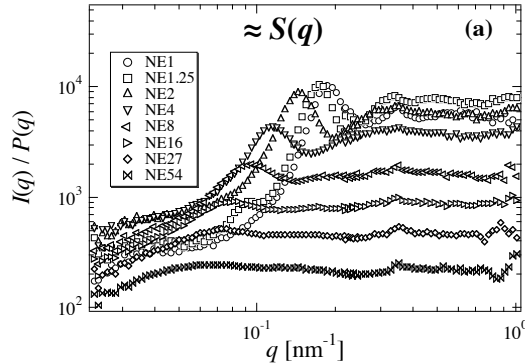
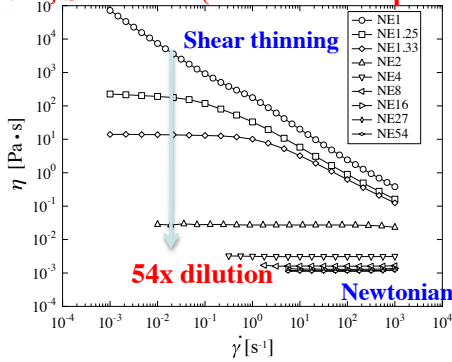
with small amount of anionic surfactant
obtained by high-pressure extrusion



Transmission micrograph

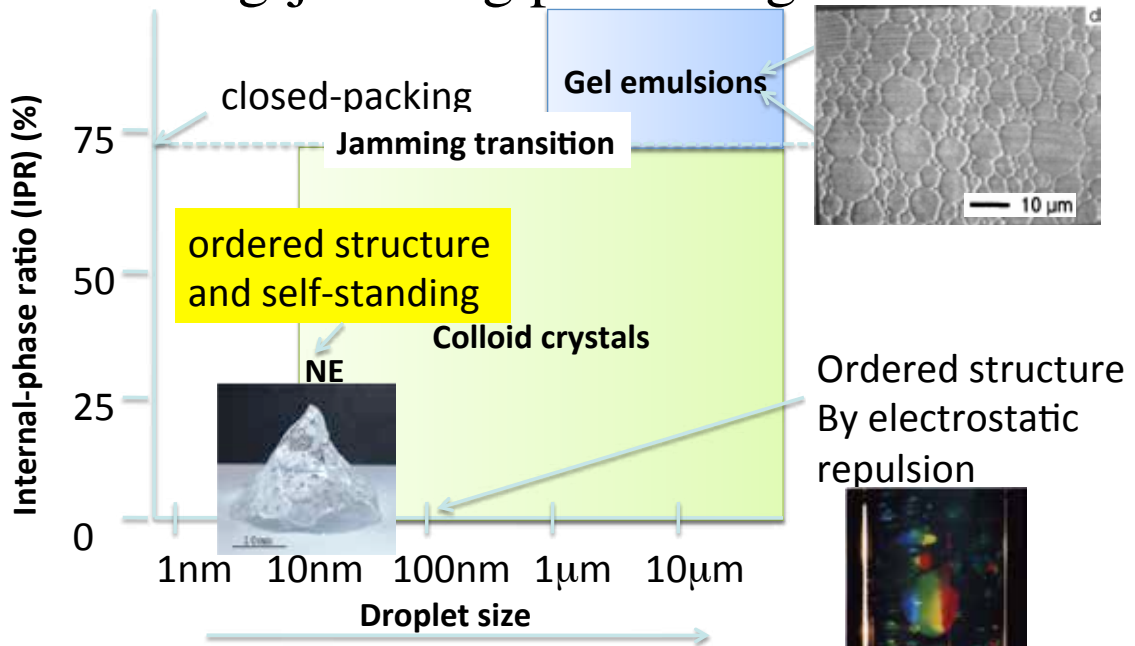
Rheological behavior

NE1; Stock soln. (ca. 25% oil-droplet dispersion)



11

Ordering-jamming phase diagram



Needs high purification of dispersoid to increase the Debye screening length

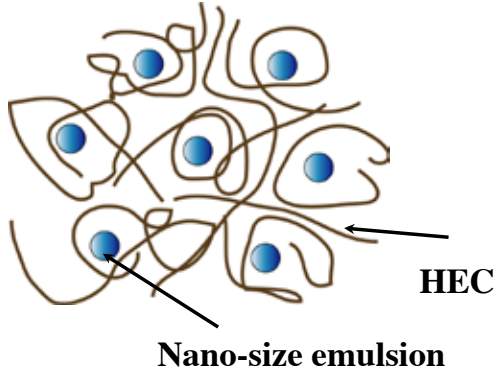
$\phi = 0.000829$
 $d = 110\text{nm}$

12

NE/polymer shake gel system: sample

J. Chem. Phys., 2007, 127, 144507

Shake gels, composed of a mixed solution of polymer and nano-size emulsion, show both **shear thinning** and **shear thickening** behaviors.



Nano-emulsion was made by high pressure extrusion of 30 wt % glycerol, 3 wt % ethanol, 16 wt % oil.

Nano-particles in the emulsion become cross-linkers to which polymer chains are attached.

Polymer : 2-hydroxyethyl cellulose (HEC) : $M_v = 1.30 \times 10^6$ g/mol
 Particle : nano-size emulsion (NE) : (Diameter ≈ 30 nm)
 Concentrations: polymer = 0.4 %, emulsion = 12 %

13

C_{NE} and C_{HEC} dependence of dilatancy

Samples

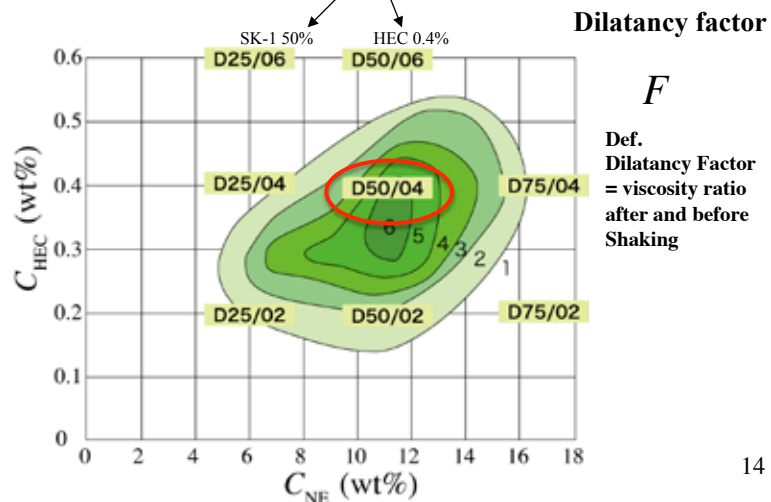
		Conc. of HEC130			dilution
		0.2%	0.4%	0.6%	
NE (wt%)	25%	D25/02 (①)	D25/04 (④)	D25/06 (⑦)	.. 4x
	50%	D50/02 (②)	D50/04 (⑤)	D50/06 (⑧)	.. 2x
	75%	D75/02 (③)	D75/04 (⑥)	—	.. 1.33x

Sample code: D50/04

Stock solution : $\approx 25\%$



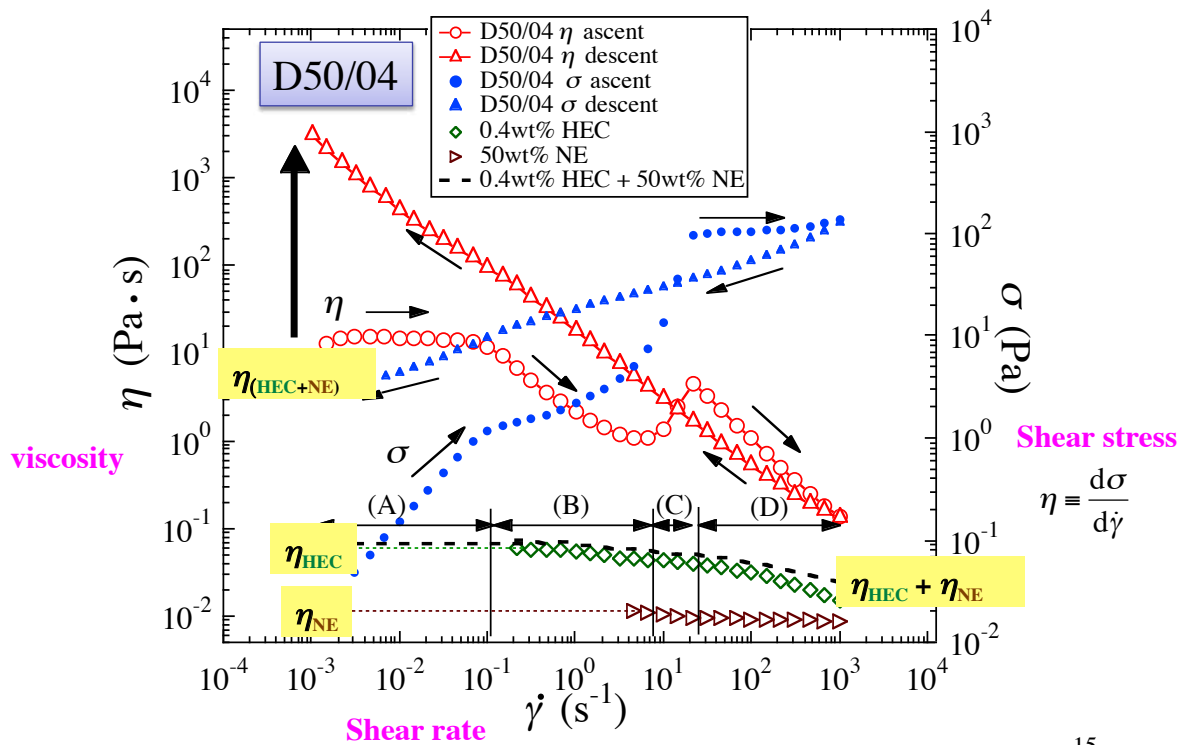
A tuning-fork vibration Viscometer (CJV5000, A&D Co. Ltd., Japan) @ 25°C, 30 Hz



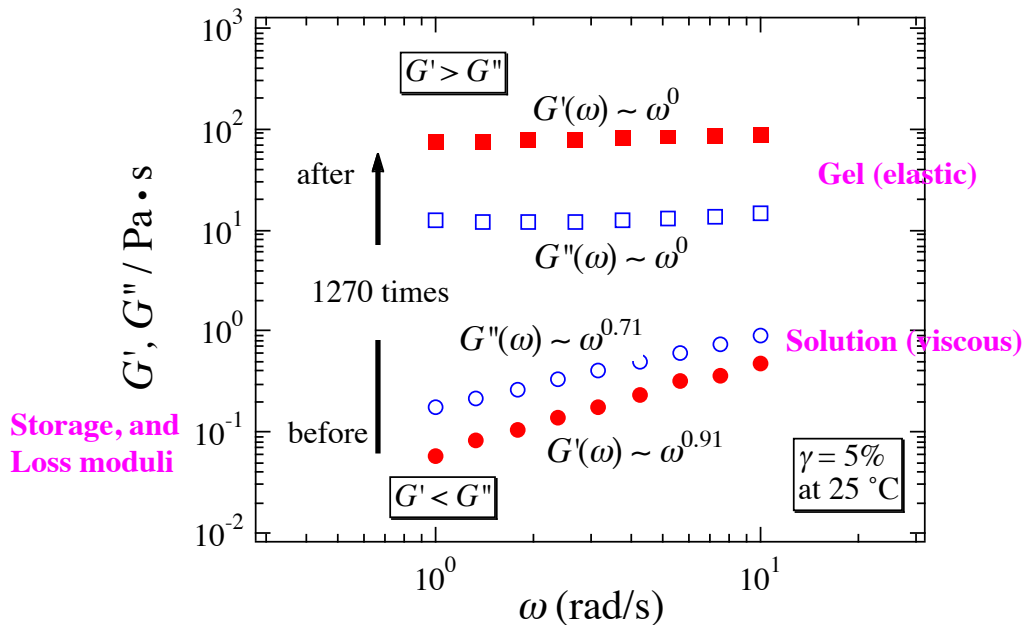
14



Flow behavior: shear-induced transition

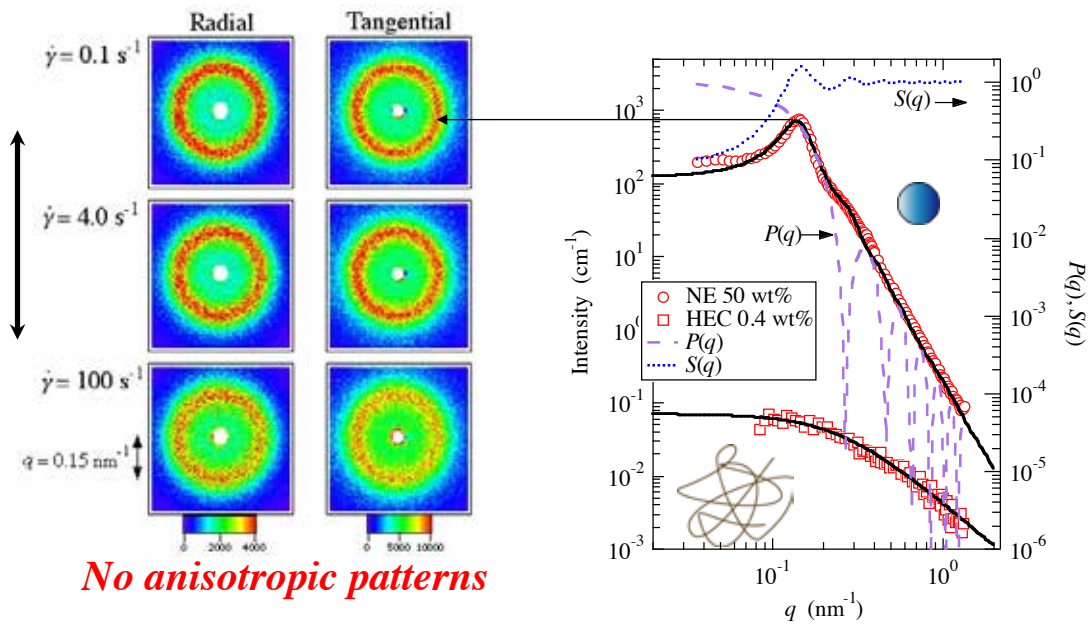


Viscoelastic transition



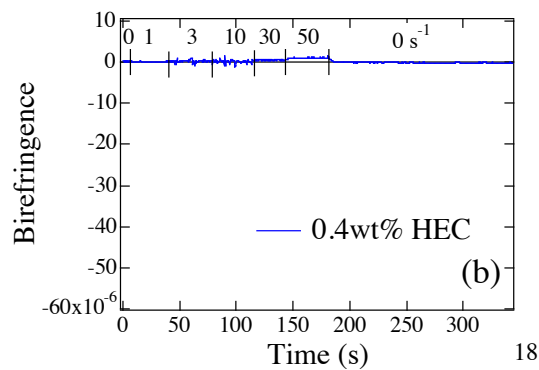
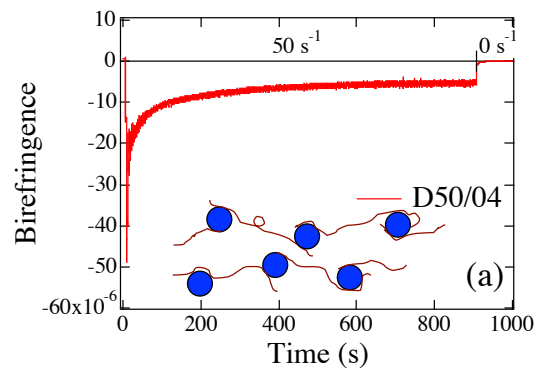
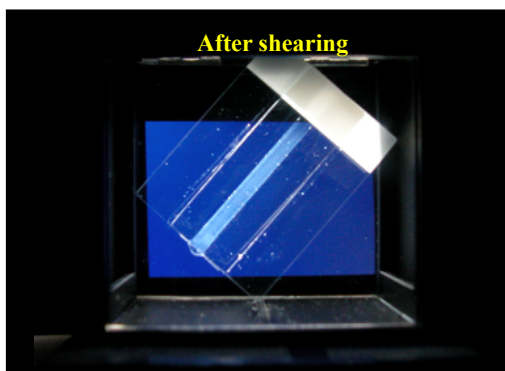
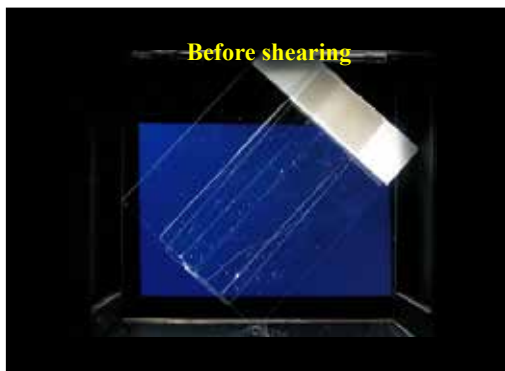
$G'(\omega)$ and $G''(\omega)$ were measured before and after shearing ($d\gamma/dt = 100 s^{-1}$ for 10 min)

2D SANS Patterns of Shake Gel

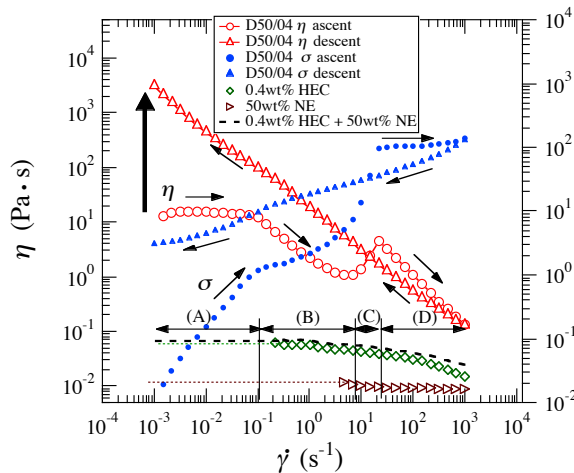


The shape of the NE and the inter-particle distance are preserved and only the long-range inhomogeneities increase by shearing.

Birefringence



Discussion 1: Intuitive interpretation



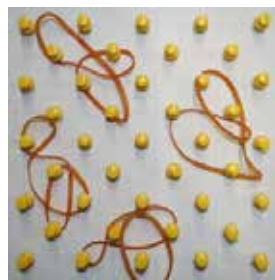
Ascent

- (A) Newtonian
- (B) Shear thinning
- (C) **Shear thickening**
- (D) Slipping

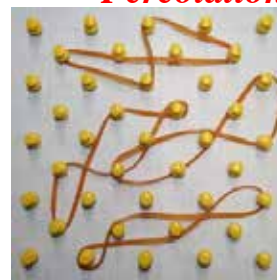
Descent and 2nd run

Dilatant behavior !!

Once a high shear is applied, the structure is formed and the relaxation time becomes very long.



Shear →



Flow direction

Percolation transition

From SANS, we know *a* does not change with shear.

Discussion 2: Estimation of shear stress at the transition

Entropy elasticity of a single Gaussian chain

$$\sigma = \frac{f}{A} = \frac{3kT}{A \langle R_0^2 \rangle^{1/2}} \frac{\langle R \rangle}{\langle R_0^2 \rangle^{1/2}} = E \frac{\langle R \rangle}{\langle R_0^2 \rangle^{1/2}}$$

Approx.1: $A \approx a^2$ $\sigma \approx \frac{f}{a^2} = \frac{3kT}{a^2 \langle R_0^2 \rangle^{1/2}} \frac{\langle R \rangle}{\langle R_0^2 \rangle^{1/2}}$

$G = E/3, \langle R \rangle / \langle R_0^2 \rangle^{1/2} \rightarrow \gamma$

$$\sigma = G\gamma = \frac{kT}{a^2 \langle R_0^2 \rangle^{1/2}} \frac{\langle R \rangle}{\langle R_0^2 \rangle^{1/2}} = \frac{kT}{a^2 \langle R_0^2 \rangle^{1/2}} \gamma$$

Approx.2: $\gamma \approx 1$

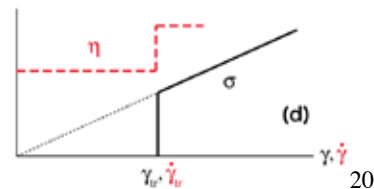
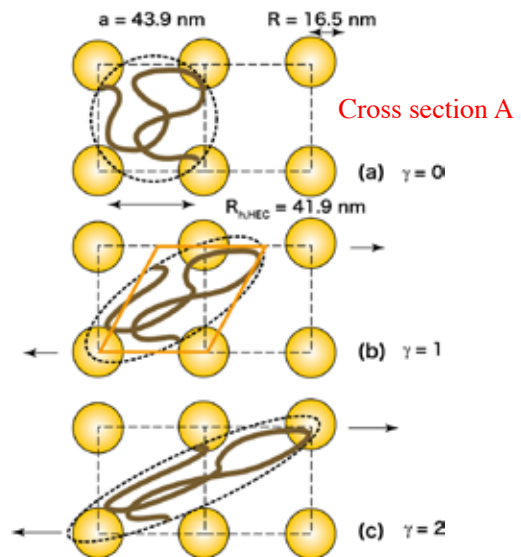
$$\sigma_{tr} = G\gamma \approx \frac{kT}{a^3}$$

$\sigma_{tr} = 45.7 \text{ [J/m}^3 = \text{Pa]}$

Predicted by SANS data only

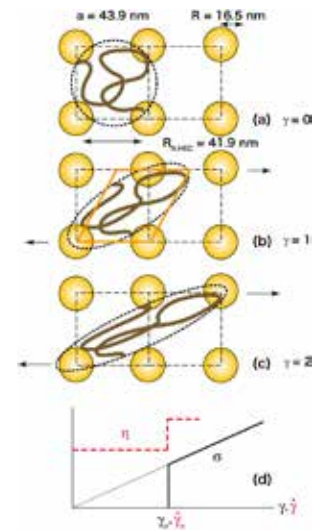
$\sigma_{tr} = 37.3 \text{ [J/m}^3 = \text{Pa]}$

← Rheology



Summary 1: NE/HEC mixture

- Shear-induced gelation in a mixture of NE and HEC was investigated by Rheo-SANS.
- The mixture exhibits a distinct viscosity-jump (dilatancy) at the shear rate of 4 s^{-1} , which corresponds to a steep upturn of SANS intensity at the low q -region.
- **No anisotropy** was observed even at the shear rate of 100 s^{-1} .
- The dilatancy effect becomes largest when $a \approx R_h$.
- The shear stress at the transition can be simply estimated **only with the structure parameters**.
- The dilatancy behavior is due not to non-Gaussian chains, but to percolation transition of the system.



Shibayama, et al., *J. Chem. Phys.*, 2007, 127, 144507.

21

Tree topics

Part I: NE/HEC Shake gel

Part II: Shear thickening of Clay/PEO

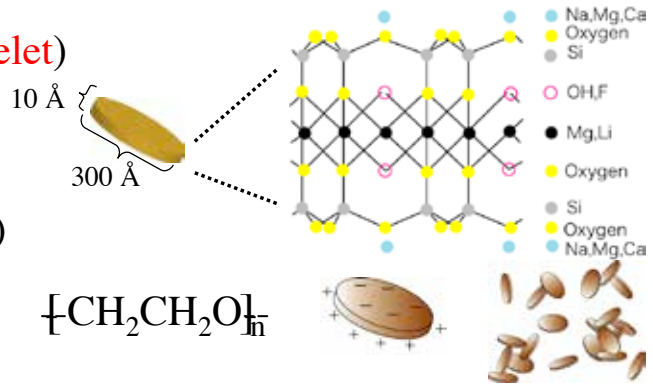
Part III: Phantom chains of CTAB/salt

shake gel composed of clay-PEO mixture

Takeda, et al., *Macromolecules*, 2010, 43, 7793.

samples

- Laponite (XLG) (clay platelet)



- poly(ethylene oxide) (PEO)

$$M_w = 400,000$$



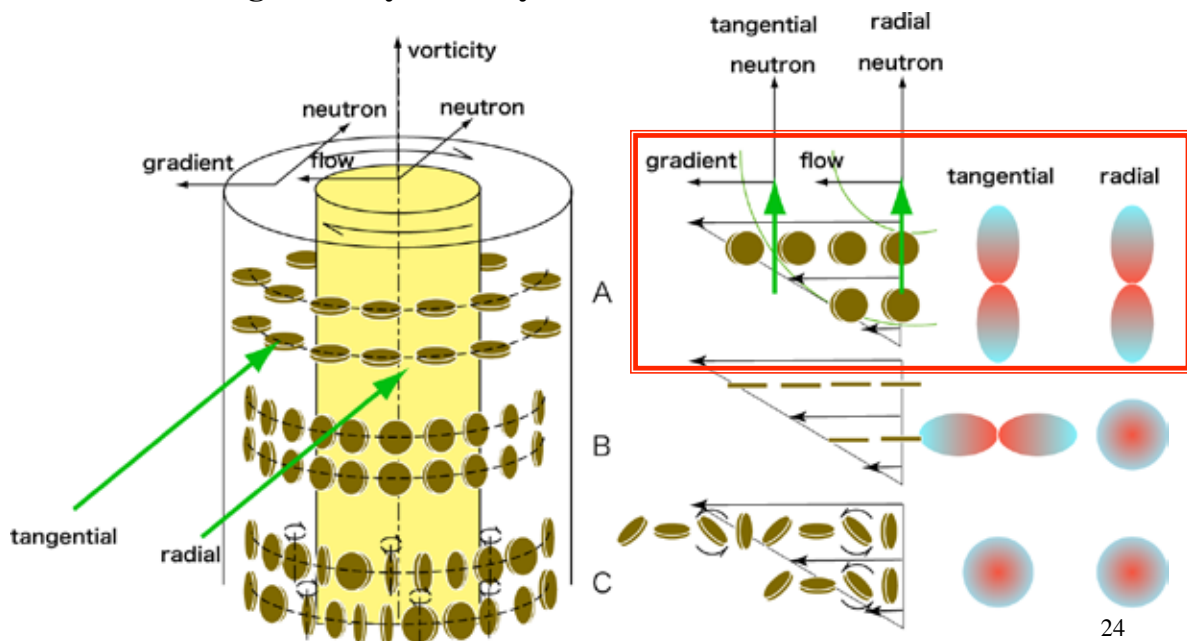
- water H₂O and D₂O mixtures for SANS (contrast variation SANS)



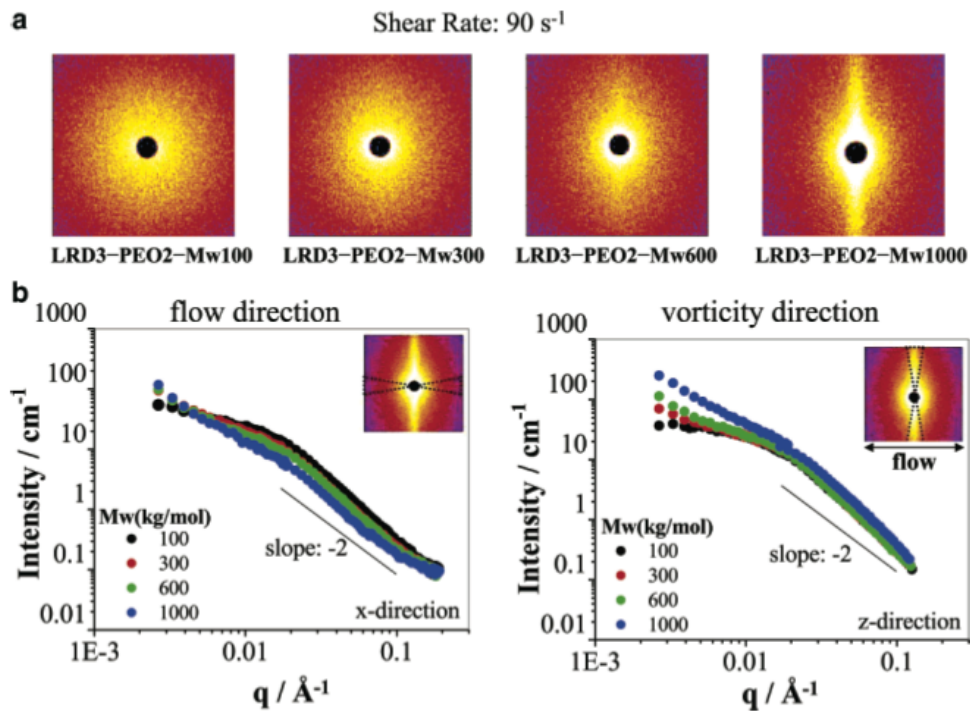
Clay Orientation in a flow field

“Gedankenexperiment”

Schematic illustration showing the relationship between the anisotropy of scattering intensity and clay's orientation.

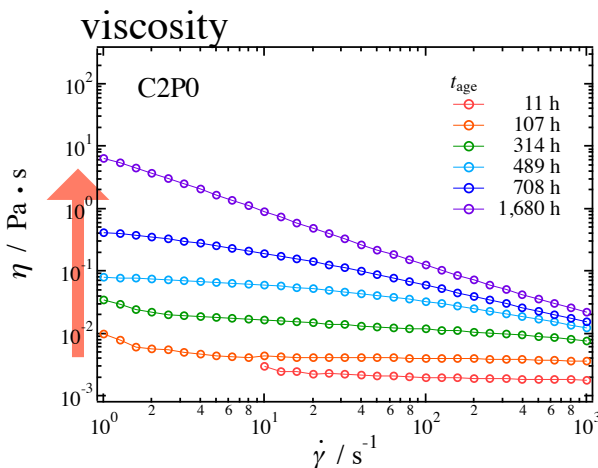


Rheo-SANS of clay/PEO



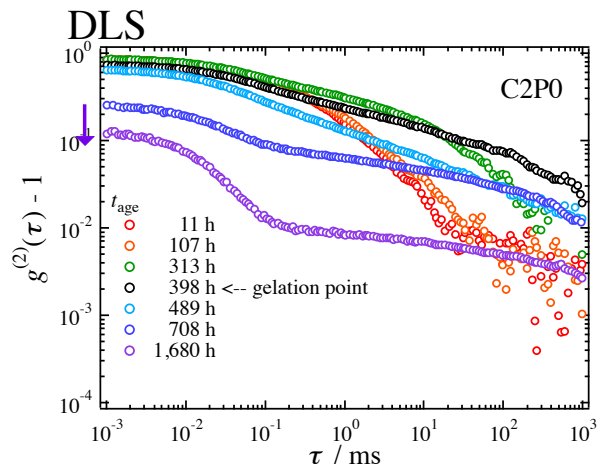
Schmidt et al., *Macromolecules*, 2005

Aging of clay 2 wt%



$\eta (\dot{\gamma} \rightarrow 0)$

Gelation at stationary state



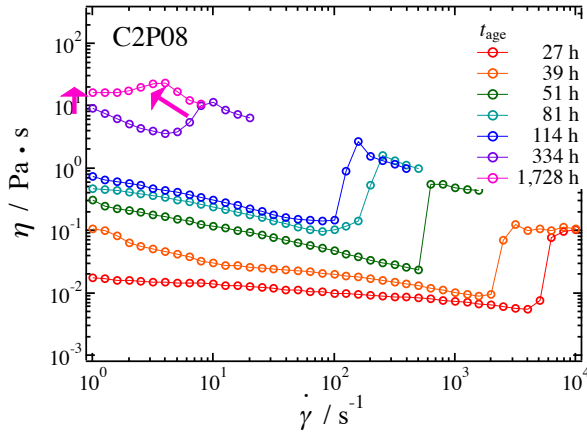
solution; $g^{(2)}(0) = 1$

Gel point; power law with τ
 → self-similar cluster formation

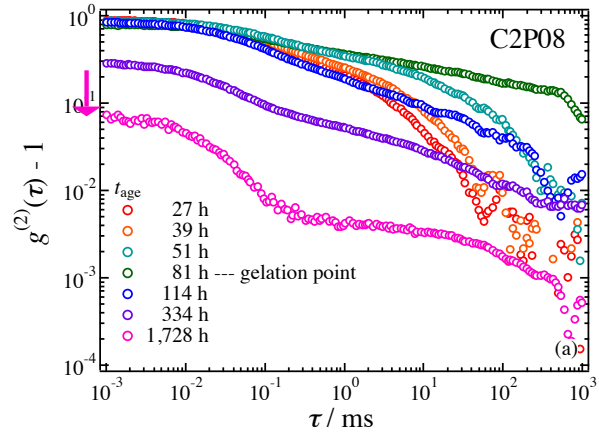
gel; suppression of $g^{(2)}(0)$
 → gel mode, nonergodicity

Evolution of clay-PEO mixture

viscosity



DLS



1. $\eta(\dot{\gamma} \rightarrow 0)$ increase
2. Lowering of $\dot{\gamma}$ at shear thickening
3. Gelation at stationary state

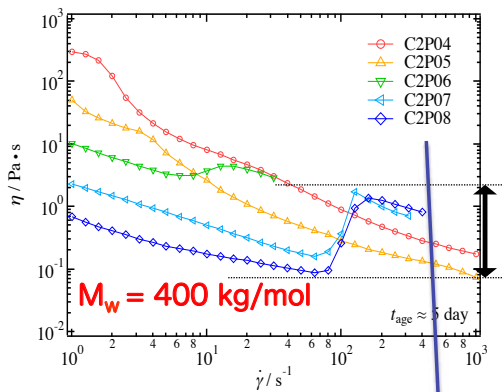
Origin of structural evolution

⇒ gelation of card-house structure of clay

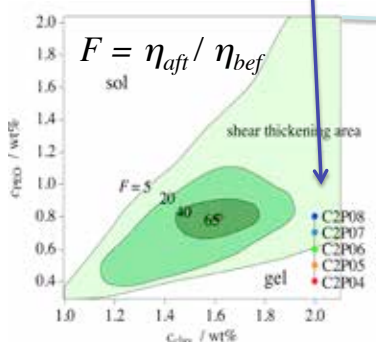
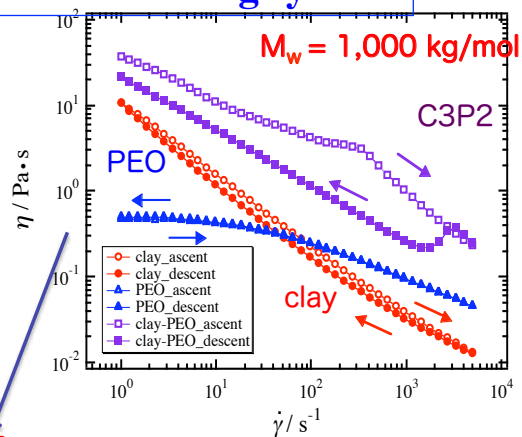
27

Rheological behaviors

shear thickening system



shear thinning system



C3P2

Matsunaga et al.,
Macromolecules, 2010, 43, 5075.

Sample code:
C2P04; clay:2 wt%-PEO:0.4 wt%

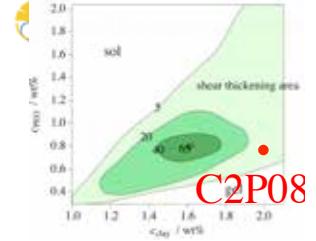
Phase diagram of shear thickening behavior with contour lines of F .

3.0%

28

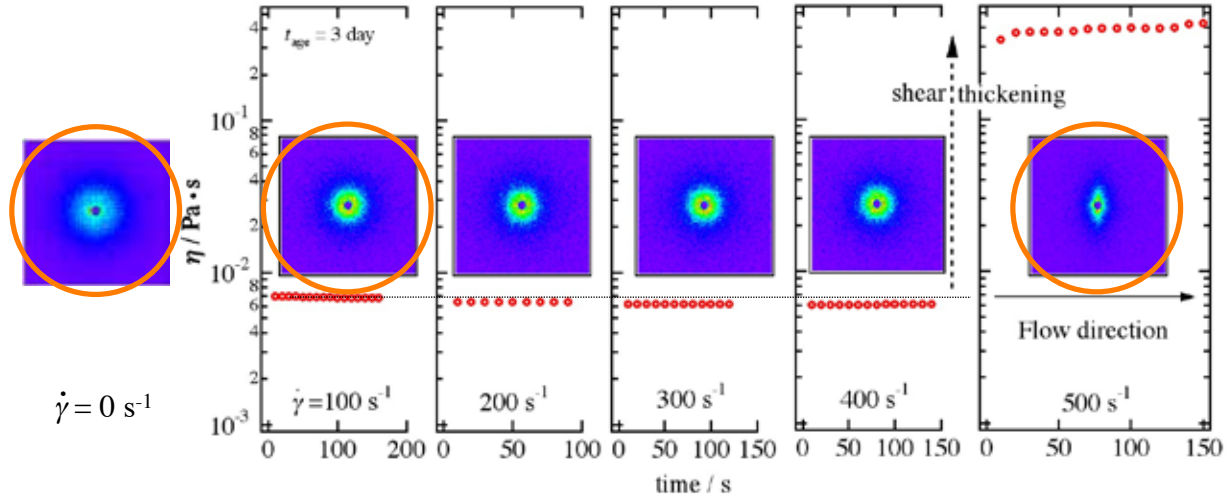


Rheology and SANS measurements



C2P08 $\phi_{D2O}=1$ $t_{age} = 3$ day

SDD = 8 m, 4m



The scattering pattern changed to anisotropic at 500 s⁻¹.

To investigate $\dot{\gamma} = 0, 100, 500$ s⁻¹ more precisely, **CV-SANS** was applied.

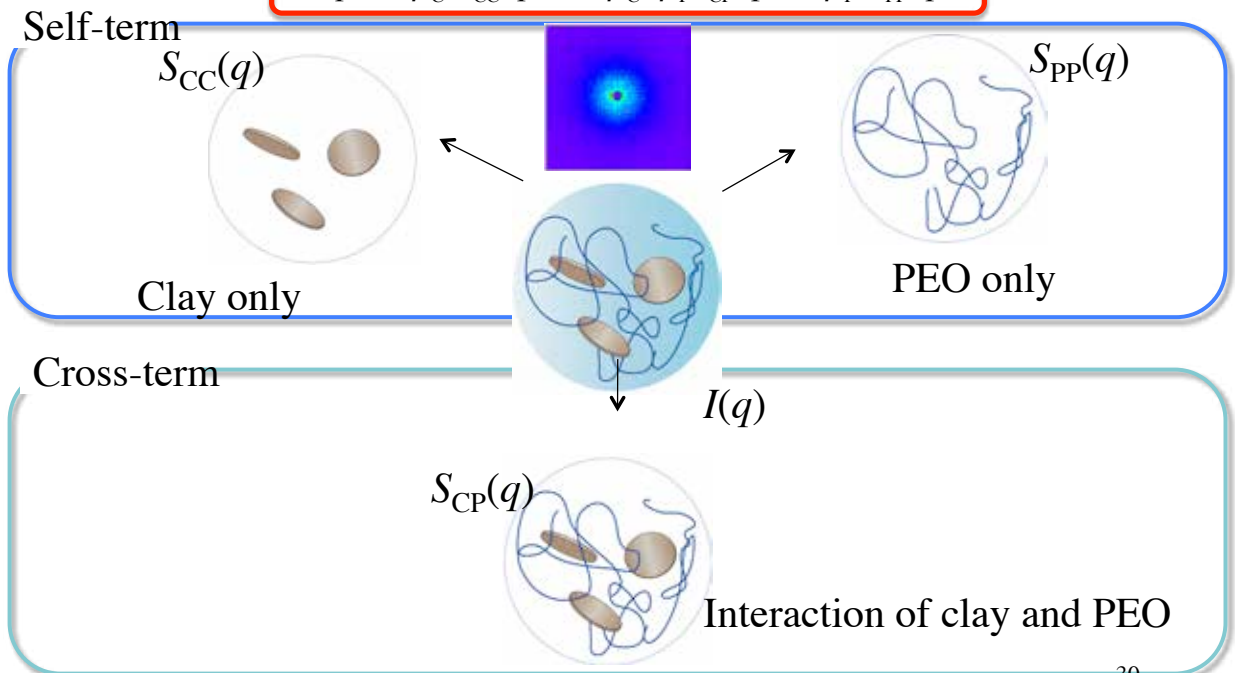
29



Scattering from three-component systems



$$I(q) \approx \Delta\rho_C^2 S_{CC}(q) + 2\Delta\rho_C\Delta\rho_P S_{CP}(q) + \Delta\rho_P^2 S_{PP}(q)$$

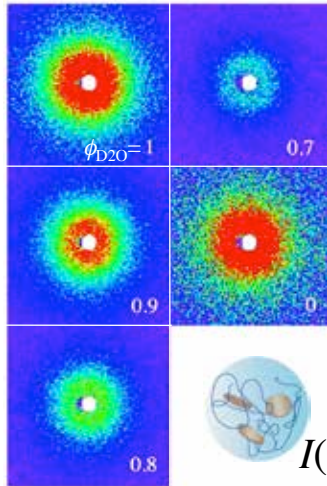
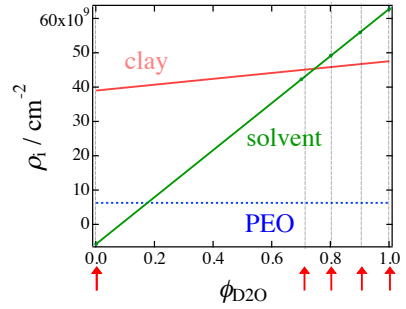
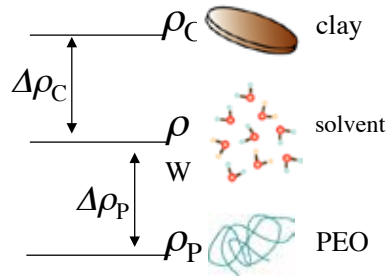


30



Contrast Variation SANS

$$I(q) \approx \Delta\rho_C^2 S_{CC}(q) + 2\Delta\rho_C \Delta\rho_P S_{CP}(q) + \Delta\rho_P^2 S_{PP}(q)$$



$I(q)$ measurements

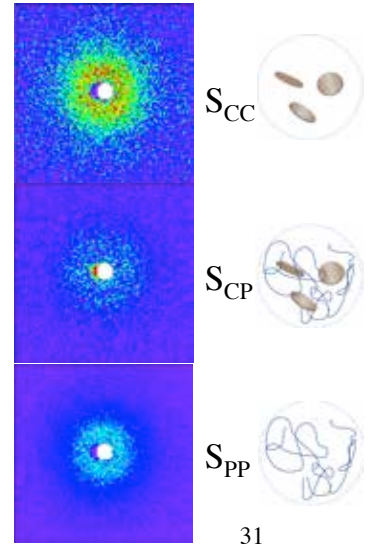
singular value decomposition

$$I_1(q) \approx {}^1\Delta\rho_C^2 S_{CC}(q) + 2{}^1\Delta\rho_C {}^1\Delta\rho_P S_{CP}(q) + {}^1\Delta\rho_P^2 S_{PP}(q)$$

$$I_2(q) \approx {}^2\Delta\rho_C^2 S_{CC}(q) + 2{}^2\Delta\rho_C {}^2\Delta\rho_P S_{CP}(q) + {}^2\Delta\rho_P^2 S_{PP}(q)$$

$$I_3(q) \approx {}^3\Delta\rho_C^2 S_{CC}(q) + 2{}^3\Delta\rho_C {}^3\Delta\rho_P S_{CP}(q) + {}^3\Delta\rho_P^2 S_{PP}(q)$$

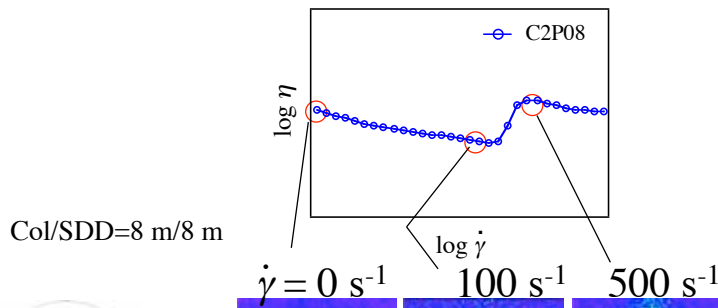
⋮



Partial scatt. fun.

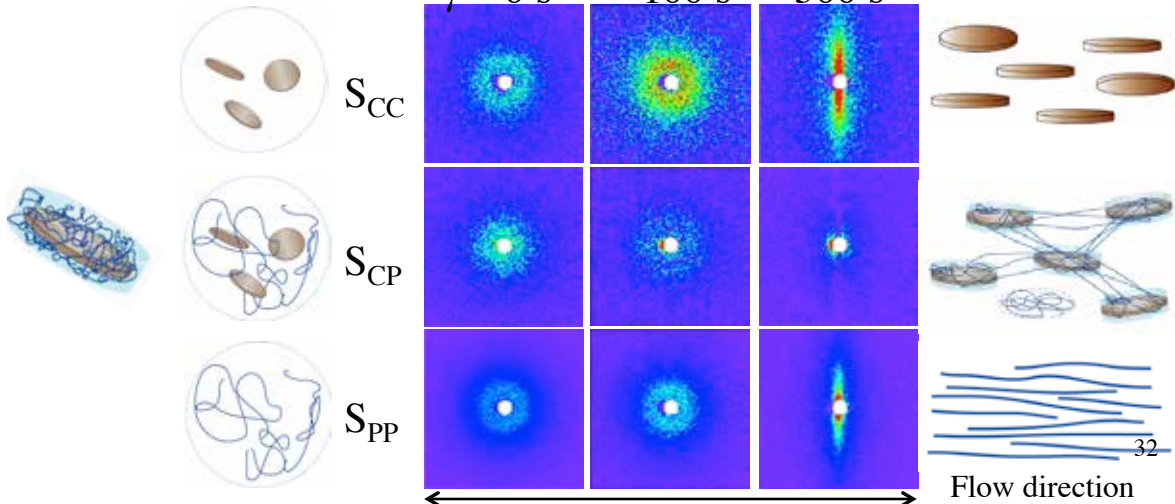


2D scattering Functions for C2P08



Col/SDD=8 m/8 m

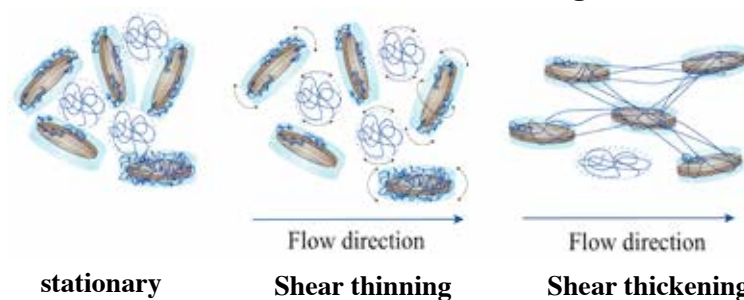
$\dot{\gamma} = 0 \text{ s}^{-1}$ 100 s^{-1} 500 s^{-1}



Conclusion 2: Clay/PEO

- Structural analyses were conducted on a clay/PEO mixture C2P08 undergoing shear thickening.
- Orientation of clay and polymer chains in C2P08 with **shear thickening** was observed by means of Rheo-SANS and Rheo-BF.
- **CV-Rheo-SANS** result revealed the origin of orientation at shear thickening threshold.
- Both of clay and PEO were orientated parallel to the flow direction.
- CV-Rheo-SANS data gave **not only the information of orientation but also that of clay-PEO interaction**.
- PEO chains adsorbed on clay surfaces are peeled off with shear thickening and bridge clay platelets, resulted in **percolation transition**.

Mechanism of shear thickening



33

Takeda, et al., Macromolecules, 2010, 43, 7793.

Tree topics

Part I: NE/HEC Shake gel

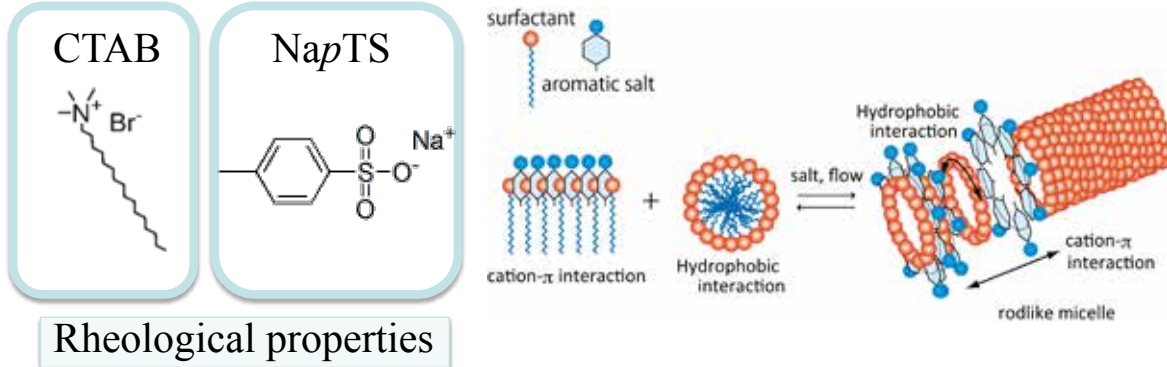
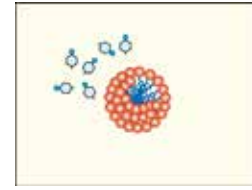
Part II: Shear thickening of Clay/PEO

Part III: Phantom chains of CTAB/salt

CTAB/NapTS

Takeda et al., Langmuir, 2011, 27, 1731.

Cetyltrimethylammonium bromide (CTAB) transforms to a rodlike structure by adding sodium *p*-toluene sulfonate (NapTS)



1. Maxwell model with a single relaxation at high micelle C .
2. shear thinning at high micelle C
3. shear thickening at low micelle C

35

Critical chain length (rod radius)

$$l_c \leq l_{\max} \approx (0.154 + 0.1265n)$$

l_c : critical chain length

l_{\max} : extended chain length

n : number of carbon



Tanford, C., (1973,1980) *The Hydrophobic Effect*, Wiley, New York.

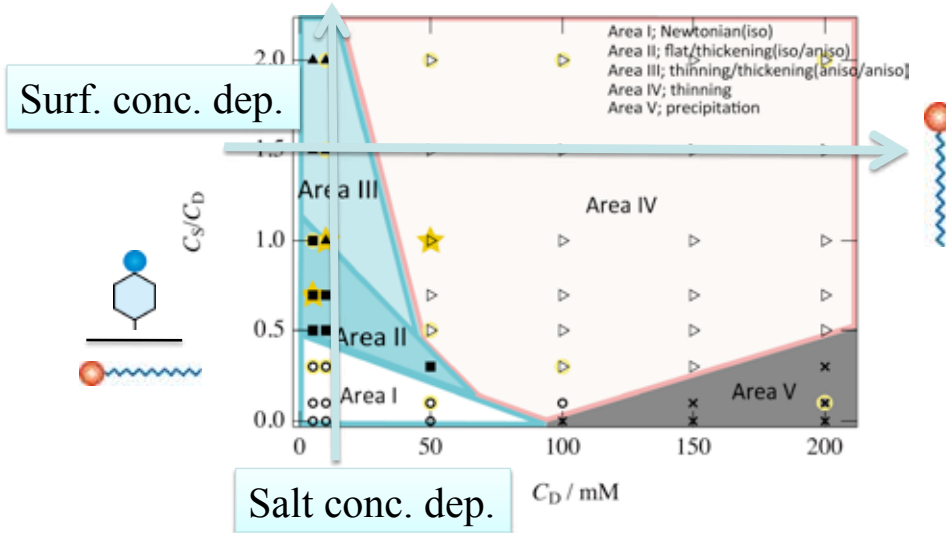
CTAB \rightarrow $l_{\max} = 21.78 \text{ \AA}$

Fitting result $R \approx 23 \text{ \AA}$

36

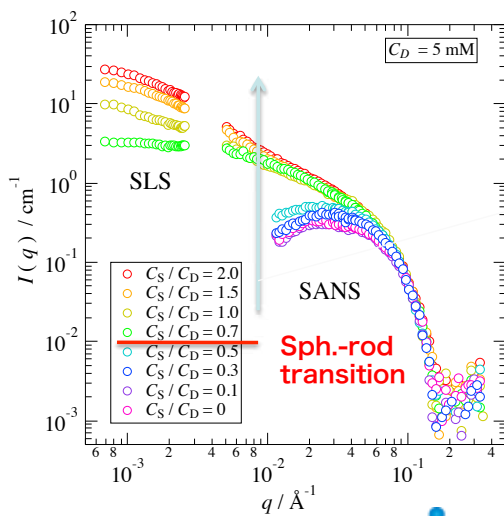
SANS at stationary state

Measuring condition
 CTAB conc. (C_D); 5~200 mM
 Salt conc. (C_S)/CTAB conc. (C_D) ratio; 0~2.0
 Room temp. (25 °C)

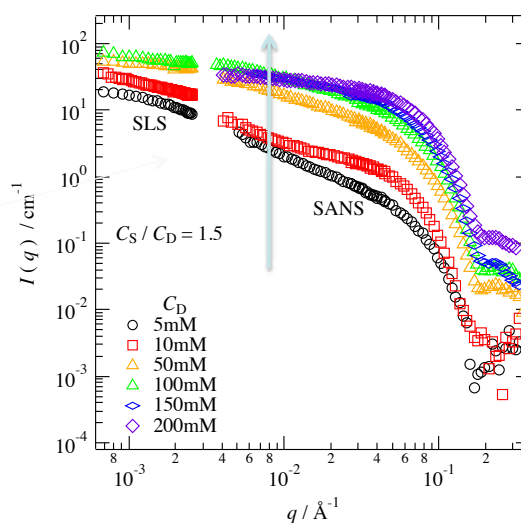
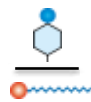


37

SANS at stationary state



Salt conc. dep.



Surfactant conc. dep.



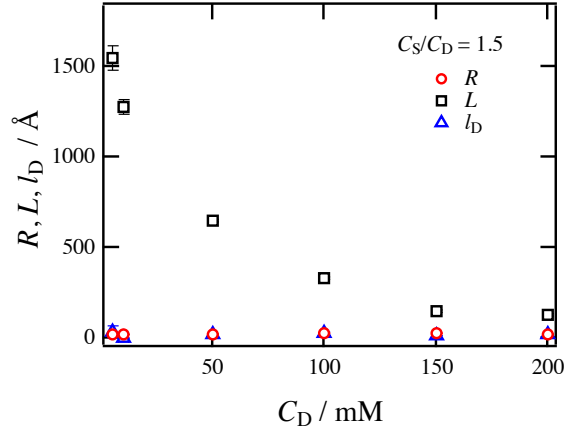
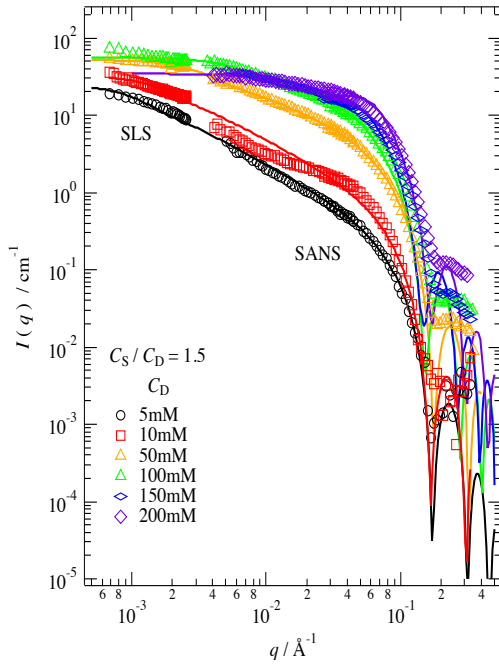
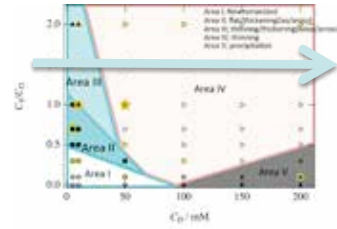
sph.-rod transition

Inter-rod interference

38



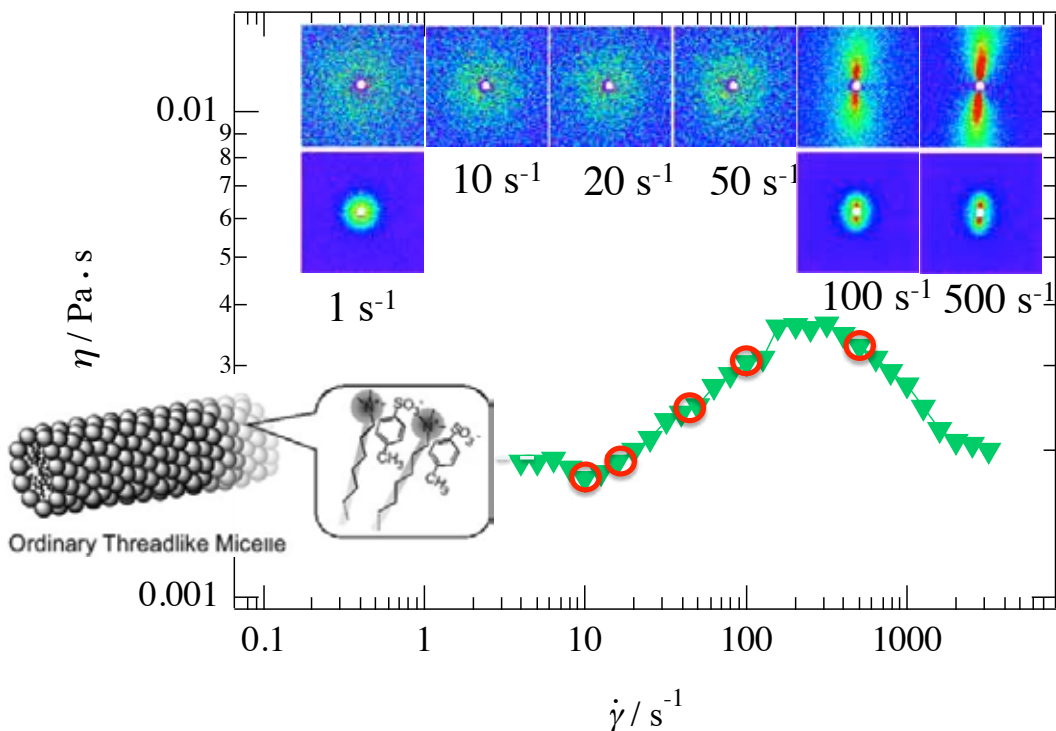
Surfactant conc. Dep.



With increasing C_D , L decreases, l_D ; constant
 → NO., no shortening, but ³⁹ **inter-rod entanglements**

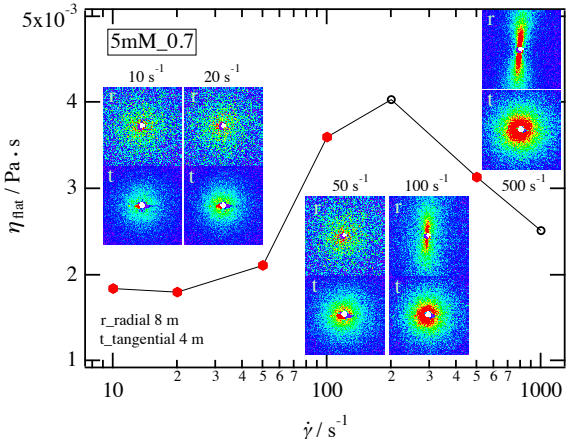
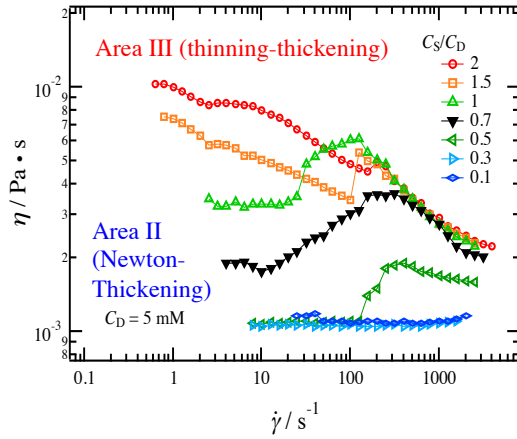
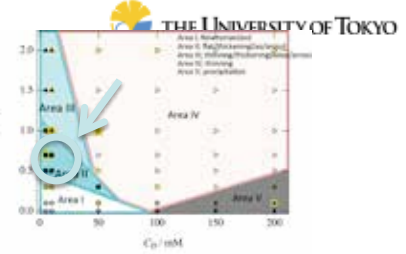


Viscosity and 2D scattering pattern on 5 mM_0.7





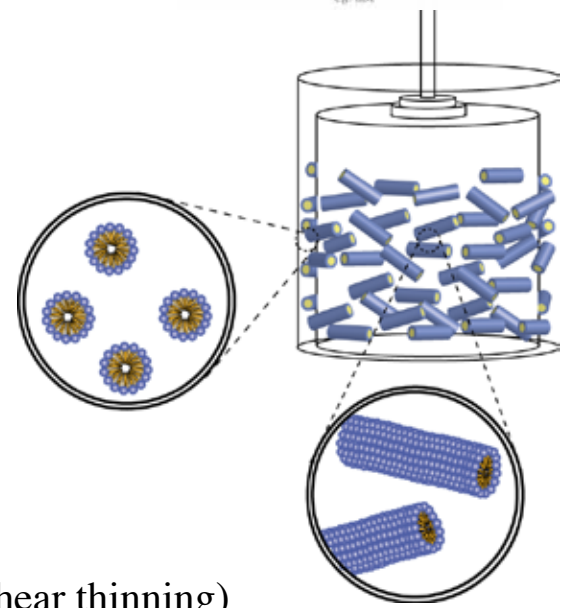
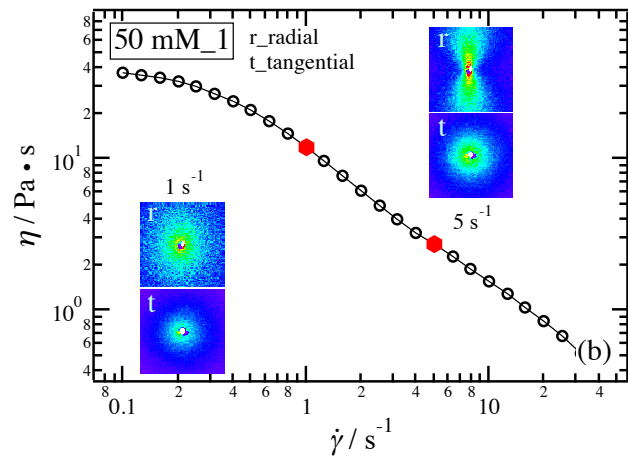
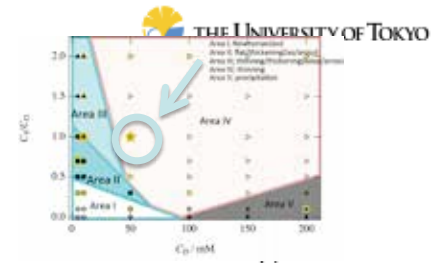
Shear thickening (low micelle conc.) Area II, III



5mM; too low conc. for entanglement formation.
Micelle orientation occurs with thickening.

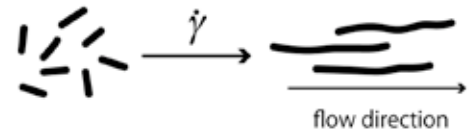
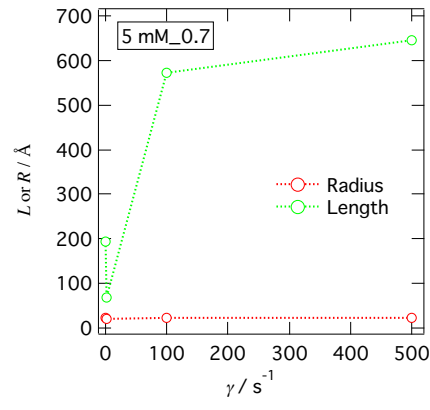
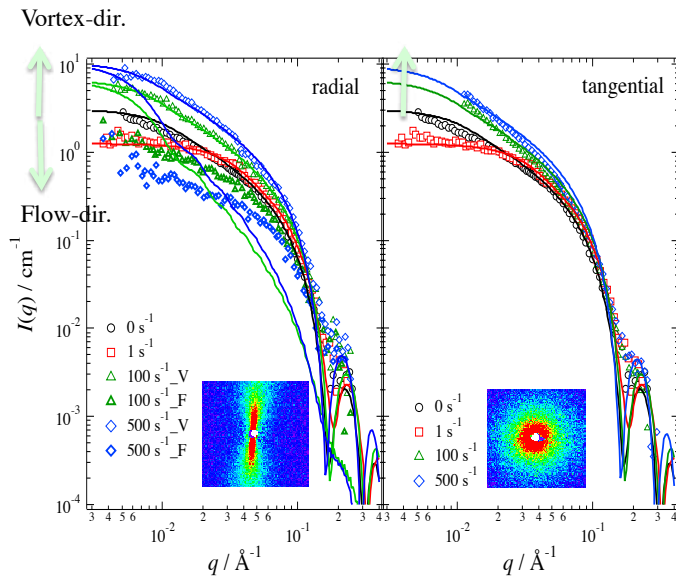


Shear thinning (high micelle conc. region) Area IV



Orientation of rodlike micelle
at high micelle conc. Region (Shear thinning)

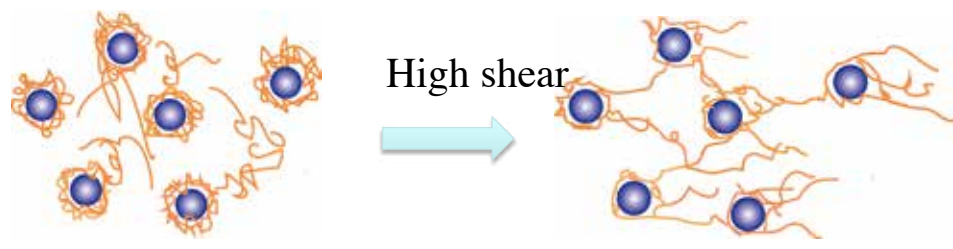
Rheo-SANS and fitting



Comparison of Shear thickening mechanisms

Particle-polymer

Bridging of particles by polymer chains



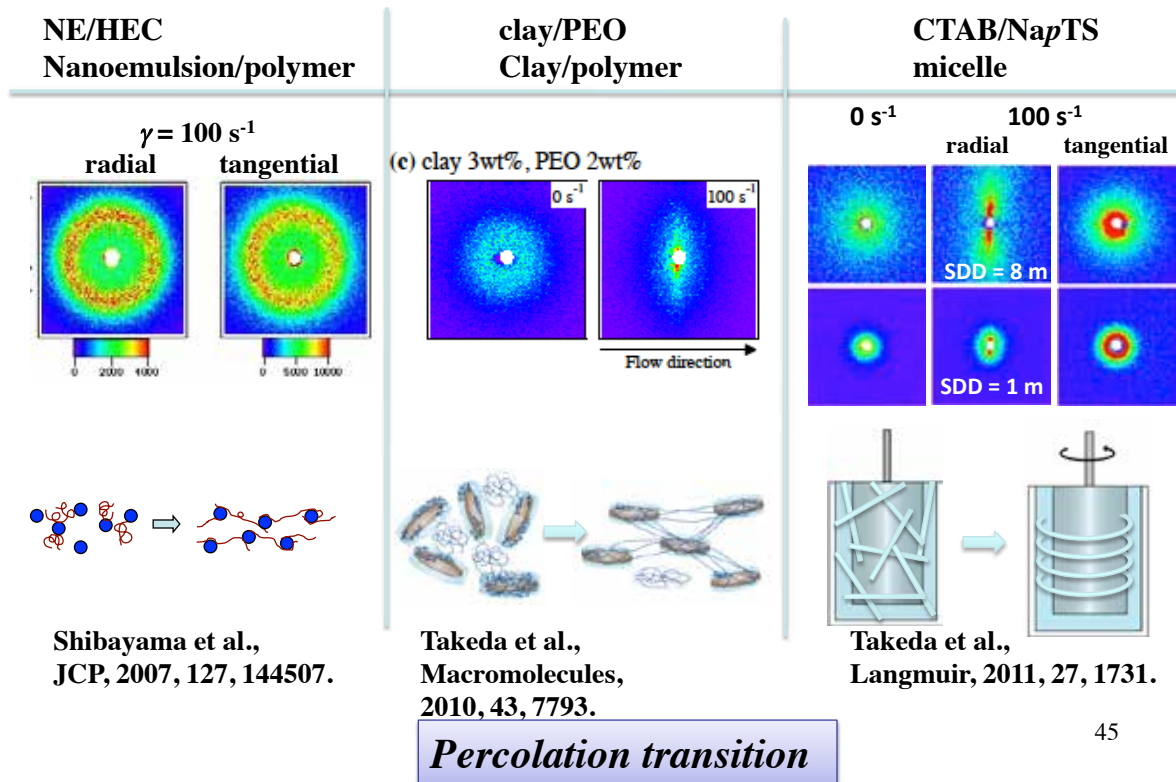
Surfactant-salt

Connection-extension



“parcolation” transition

Summary: Rheo-SANS of Shear thickening



45

Conclusion

Shear-thickening phenomena were investigated by Rheo-SANS for complex systems, i.e., nano-emulsion/polymer, clay/polymer, and surfactant/salt aqueous systems.

It was found that

- (1) shear-thickening occurred in a **small window of particle/polymer concentrations**, where the inter-particle distance is close to the polymer size.
- (2) Anisotropic patterns are observed by Rheo-SANS when the particles have anisotropic shape.
- (3) The transition is explained as a **percolation transition** in which polymer chains bridge neighboring particles.
- (4) In the case of CTAB/salt, a **continuity transition** is responsible for the shear-thickening behavior.

46



Acknowledgement

ISSP, The University of Tokyo

T. Matsunaga, M. Takeda, S. Miyazaki, N. Osaka, T. Nishida

JAEA

Dr. H. Endo

Beauty Care Research Labs. Kao Co., Ltd

Dr. T. Kume, H. Kawada, H. Iwai, and T. Sano

(nano-emulsion)

Nagaoka University of Technology,

Prof. T. Takahashi

(rheo-birefringence measurement)

*** Ministry of Education, Science, Sports and Culture, Japan**

(Grant-in-Aid for Scientific Research (A), 2006-2008, No. 18205025,

and for Scientific Research on Priority Areas, 2006-2010, No. 18068004)

*** SANS experiment: NSPAC, ISSP : Proposal No. 6558, 8620, 9599, 10627,**

47



Fitting parameter

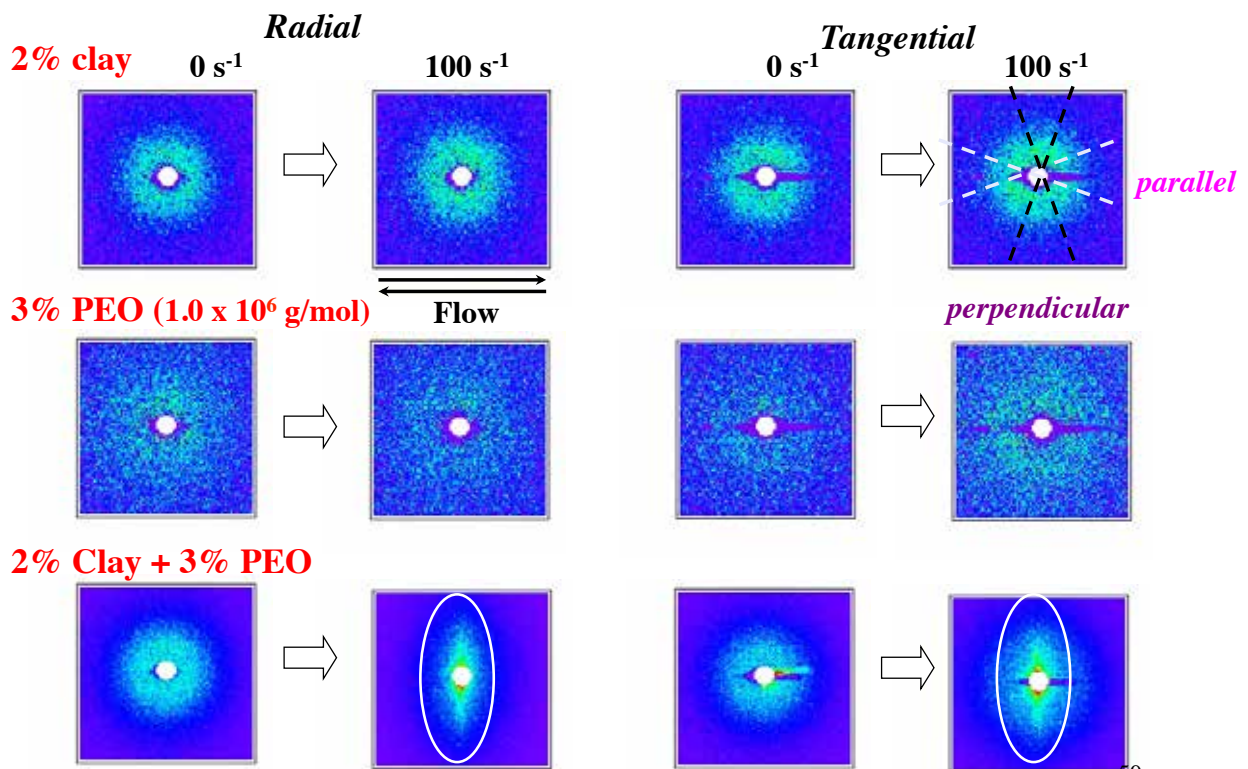
low $\xrightarrow{\text{PEO conc}}$ high

	C2P04	C2P05	C2P06	C2P07	C2P08
$R_C / \text{\AA}$			150		
$D_C / \text{\AA}$			10		
ϕ_{clay}			0.00763		
$R_{\text{PY}} / \text{\AA}$	91.1	72.1	75.9	76.0	108
$R_{\text{pl}} / \text{\AA}$	150	150	150	150	193
$D_{\text{pl}} / \text{\AA}$	17.5	20.8	20.6	21.5	24.3
ϕ_{pl}	0.235	0.388	0.378	0.298	0.206
S_{PP}^0	0.0824	0.119	0.137	0.194	0.255
$\xi / \text{\AA}$	113	117	121	127	181

Gel phase | shear thickening phase

49

Comparison: Clay-PEO



50

Acknowledgement



51

まとめ

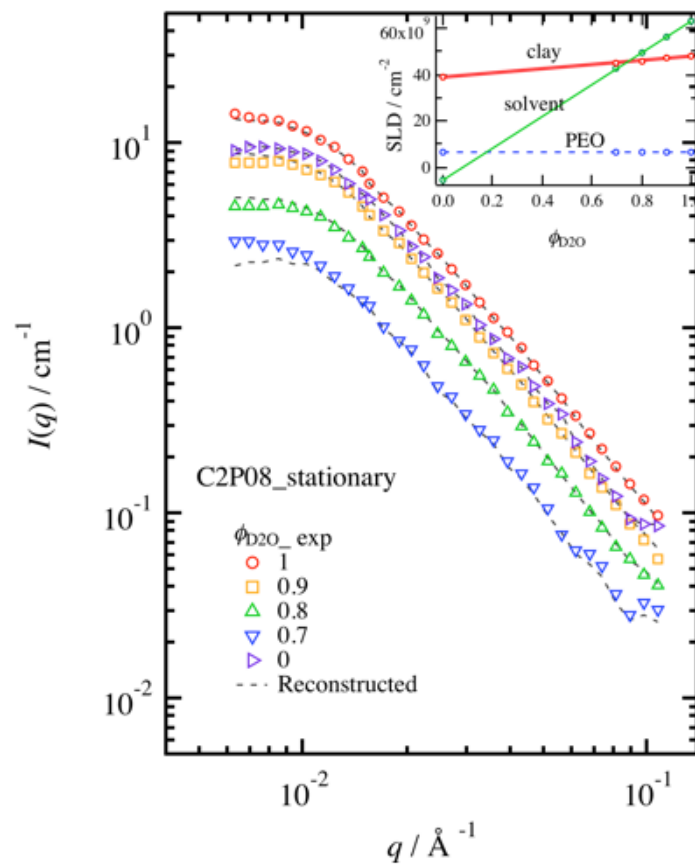
クレー-PEO高分子溶液系

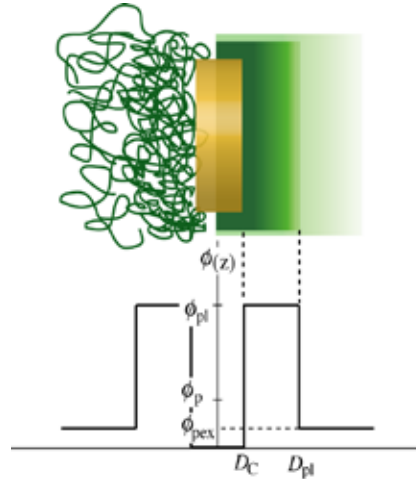
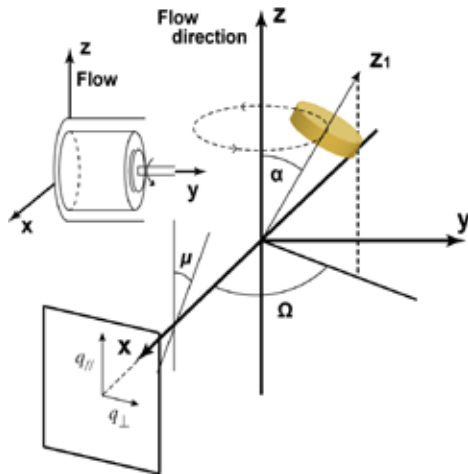
- クレー-PEO高分子溶液系においてshear thickening挙動が観察された。この時の構造変化をcontrast variation SANSにより研究し、クレーへの高分子鎖の吸着、shear thickeningはパーコレーション転移であることを解明した。

CTAB-塩混合系

- CTAB-塩混合系は粒子-高分子混合系と同様、特定濃度領域においてshear thickening挙動を示し、剪断による構造転移をすることが分かった。
- shear thickeningに伴う配向と、ミセルの伸長が確認された。この系のshear thickeningは、半径が変化していないことから紐状ミセルが剪断により流動方向に配向、連結し、より長い紐状ミセルへと転移したことで粘度増大するために起きる現象であると考えられる。

52





$$S_{CC} = \int_{\alpha=0}^{\pi/2} F_{cyl}(R_C, D_C, \alpha)^2 \sin \alpha d\alpha$$

$$F_{cyl}(R, D, \alpha) = 2V \frac{\sin(qD \cos \alpha) J_1(qR \sin \alpha)}{qD \cos \alpha \quad qR \sin \alpha}$$

☆ Structure factor : Percus-Yevick equation

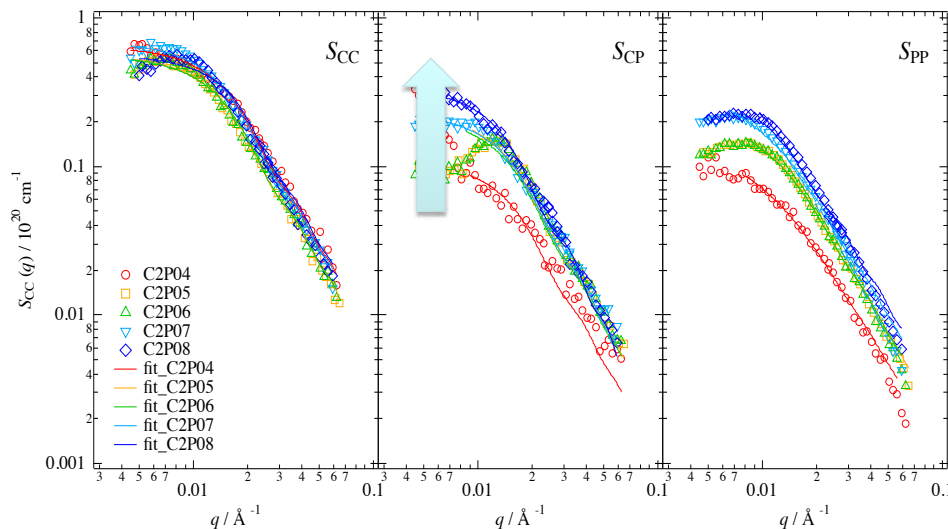
$$S_{CP} = \frac{n_C}{2} \left\{ (\phi_{pl} - \phi_{pex}) \int_{\alpha=0}^{\pi/2} F_{cyl}(R_C, D_C, \alpha) F_{cyl}(R_{pl}, D_{pl}, \alpha) \sin \alpha d\alpha - \phi_{pl} \int_{\alpha=0}^{\pi/2} F_{cyl}^2(R_{pl}, D_{pl}, \alpha) \sin \alpha d\alpha \right\}$$

$$S_{PP} = \frac{n_C}{2} \left\{ \int_{\alpha=0}^{\pi/2} [(\phi_{pl} - \phi_{pex}) F_{cyl}(R_{pl}, D_{pl}, \alpha) - \phi_{pl} F_{cyl}(R_C, D_C, \alpha)]^2 \sin \alpha d\alpha + \frac{S_{PP}^0(0)}{1 + \xi^2 q^2} \right\}$$

55

Partial Scattering Functions at 0 s⁻¹

S_{ij}(q)s at various concentrations with fitting functions



- At all conditions, S_{CC} curves show the same function.
- S_{CP} values are positive. → There are polymer condensed layer on a clay surface.
- As increasing polymer concentration, S_{CP} values increase.

56

Fitting Parameters

fitting parameter

low ← PEO concentration → high

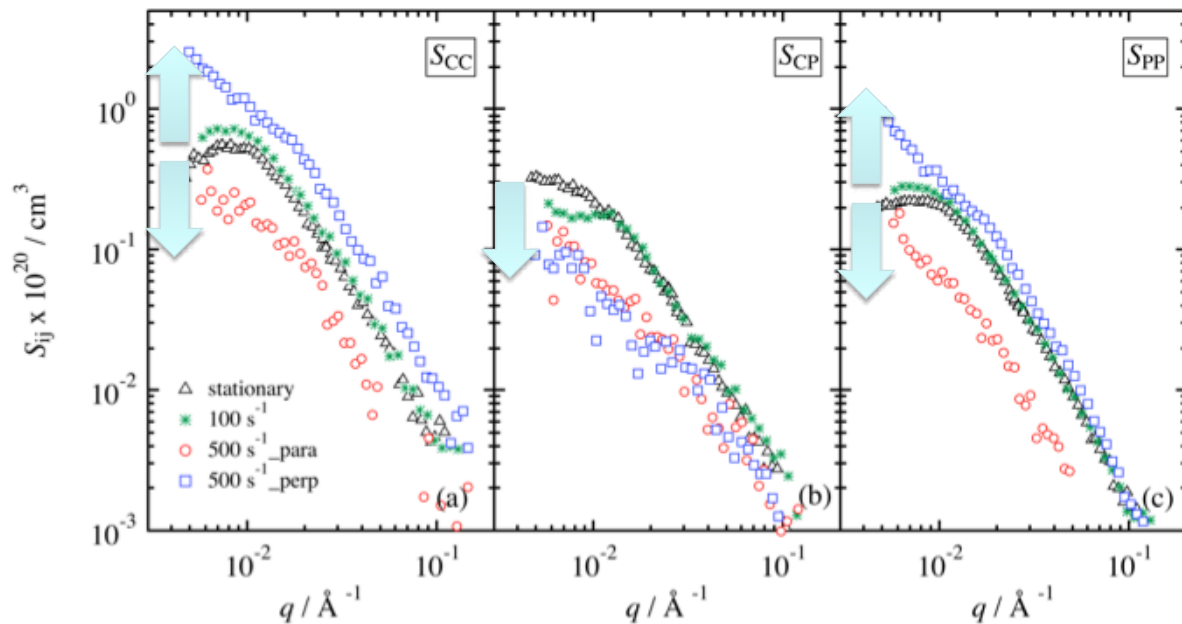
	C2P04	C2P05	C2P06	C2P07	C2P08
$R_C / \text{Å}$	150				
$D_C / \text{Å}$	10				
ϕ_{clay}	0.00763				
$R_{\text{PY}} / \text{Å}$	91.1	72.1	75.9	76.0	108
$R_{\text{pl}} / \text{Å}$	150	150	150	150	193
$D_{\text{pl}} / \text{Å}$	17.5	20.8	20.6	21.5	24.3
ϕ_{pl}	0.235	0.388	0.378	0.298	0.206
S_{PP}^0	0.0824	0.119	0.137	0.194	0.255
$\xi / \text{Å}$	113	117	121	127	181

gel area

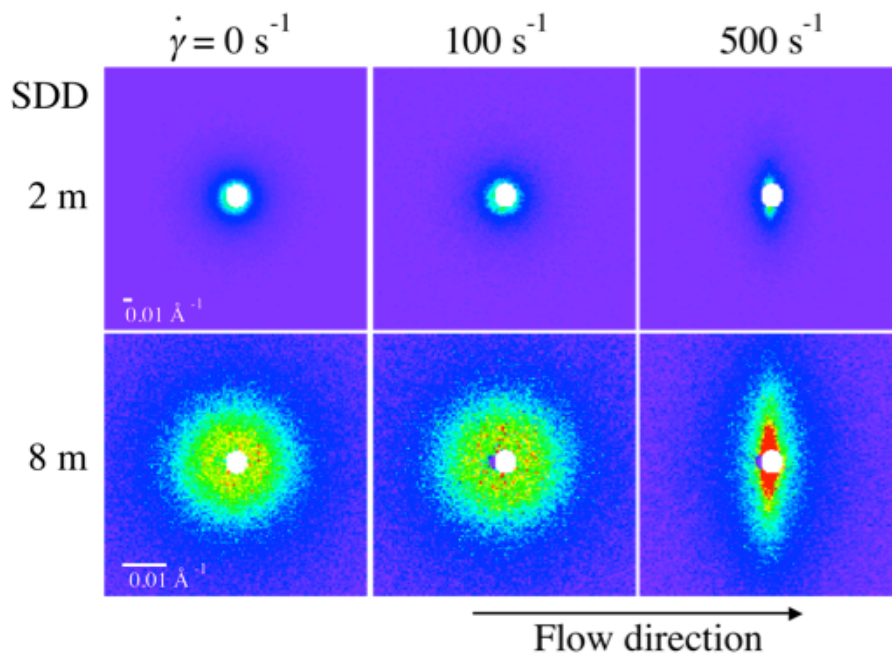
shear thickening area

There is no significant structure change on these concentrations.

57

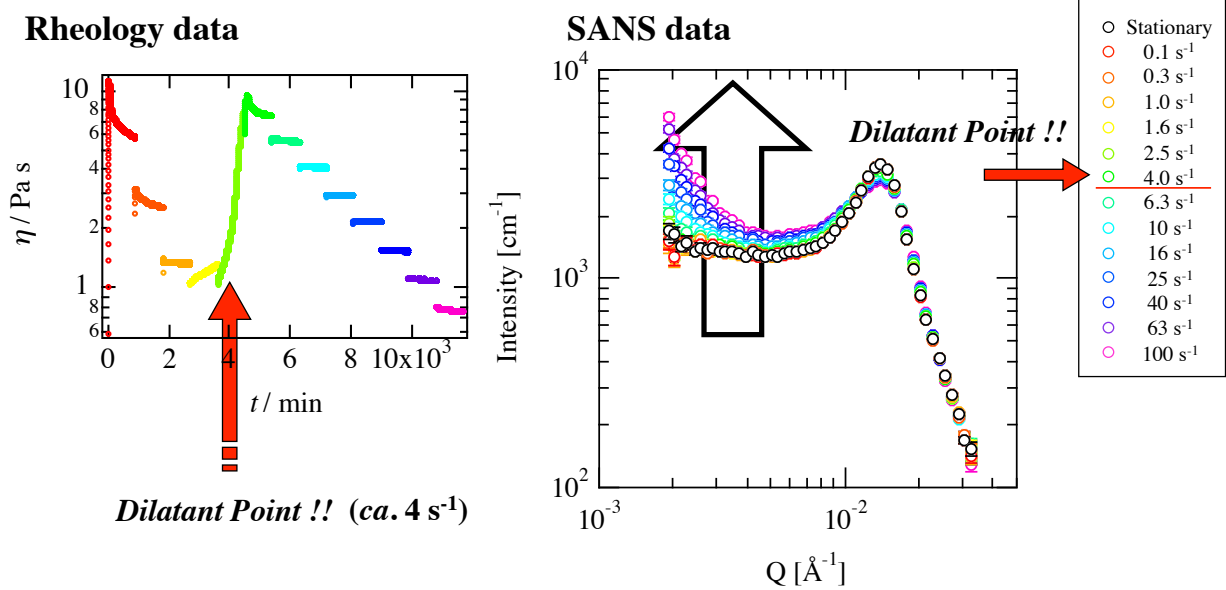


58



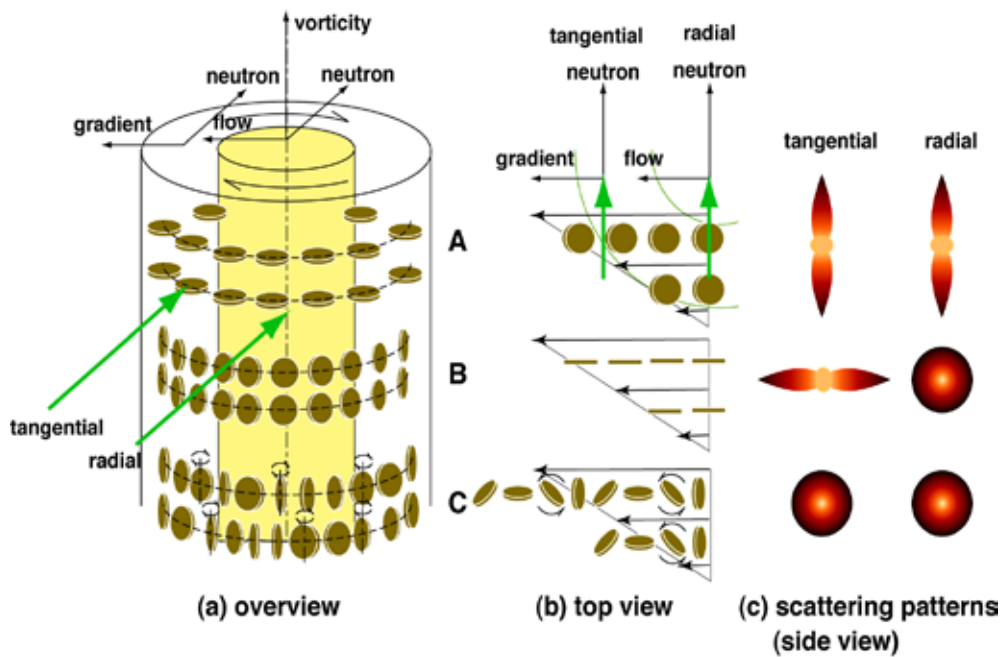
59

Rheo-SANS 1



At the shear rate above the dilatant point, a steep increase of the scattering intensity was observed in the low-Q region.

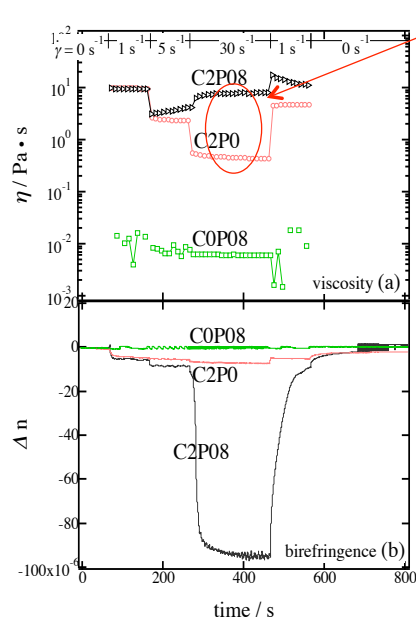
60



61

Birefringence Measurements

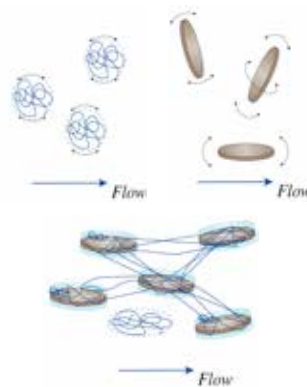
Viscosity η and birefringence Δn at various shear rates



Shear thickening

$$\dot{\gamma} = 30 \text{ s}^{-1}$$

$$t_{\text{age}} \sim 840 \text{ h}$$



Only C2P08 with shear thickening shows optical anisotropy. The changes in Δn come from clay orientation coupled with PEO.

62

Schmidtの例

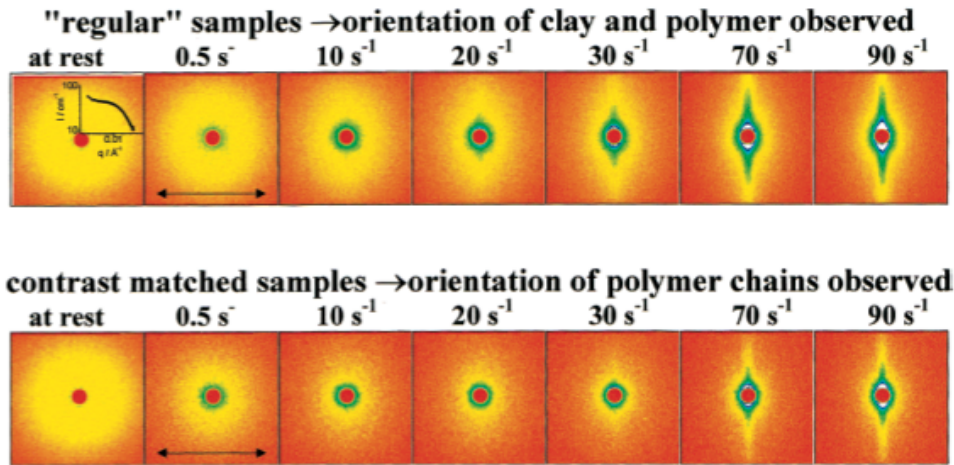
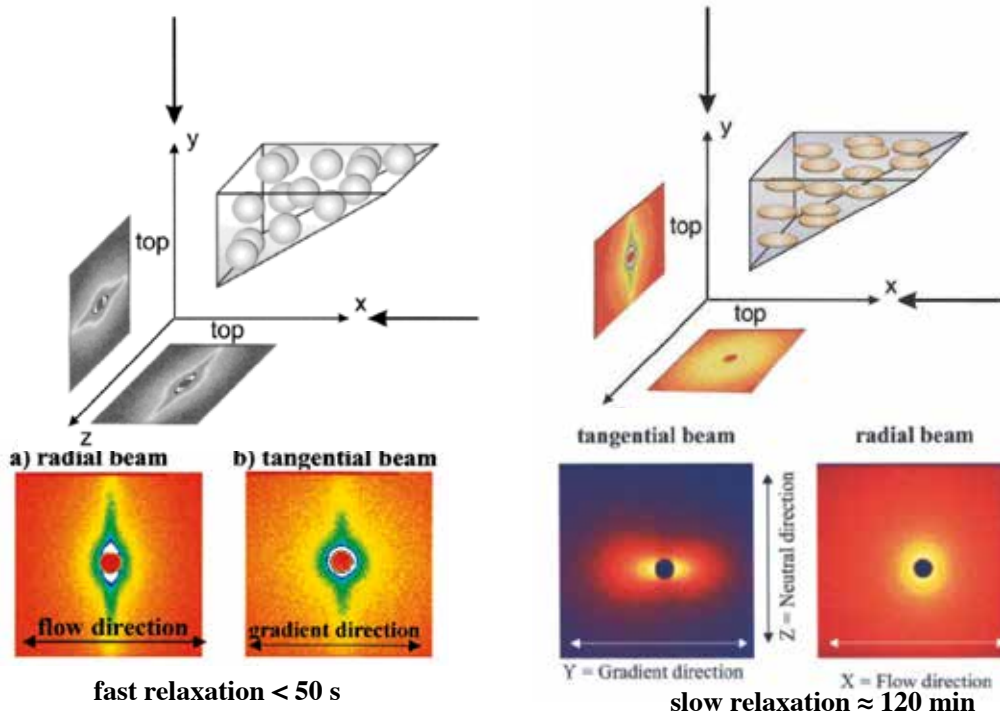


Figure 4. Radial beam configuration: two-dimensional SANS profiles obtained from LRD2 samples in D₂O (first series, same scaling) and LRD2 contrast matched samples (second series, same scaling).

Schmidt et al. *Macromolecules* 35, 2002

NIST: Two different orientations



Schmidt et al., *Macromolecules*, 2000, 2002.

JPS, 2004



Discussion 3: Effects of non-Gaussianity

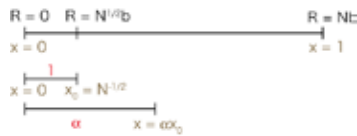
3. Effects of non-Gaussianity

For highly-stretched polymer chains, the restoring force can be expressed by the **inverse-Langevin chains**, $L^{-1}(x)$,

$$f = \frac{kT}{b} L^{-1}\left(\frac{\langle R \rangle}{Nb}\right)$$

Hence, the shear stress is given by,

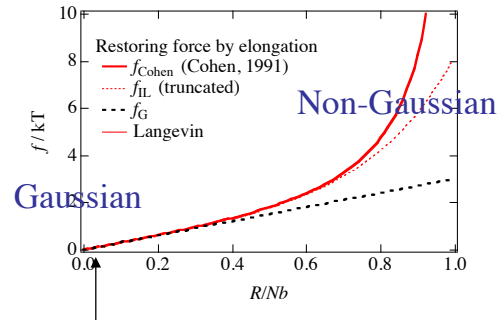
$$\sigma = G\gamma = \frac{4}{3} N^{1/2} \frac{kT}{a^2} L^{-1}\left(\frac{\gamma}{N^{1/2}}\right)$$



$$L^{-1}(x) = 3x + \frac{9}{5}x^3 + \frac{297}{175}x^5 + O(x^7)$$

$$\approx x \frac{3 - (36/35)x^2}{1 - (33/35)x^2} + O(x^6) \quad (\text{Padé approximation})$$

Since $N = 2848$, $N^{1/2}$ is order of 50 for HEC. Thus, $x \approx \gamma / N^{1/2} \approx 0.02$, where the restoring force is given by Gaussian chain statistics.

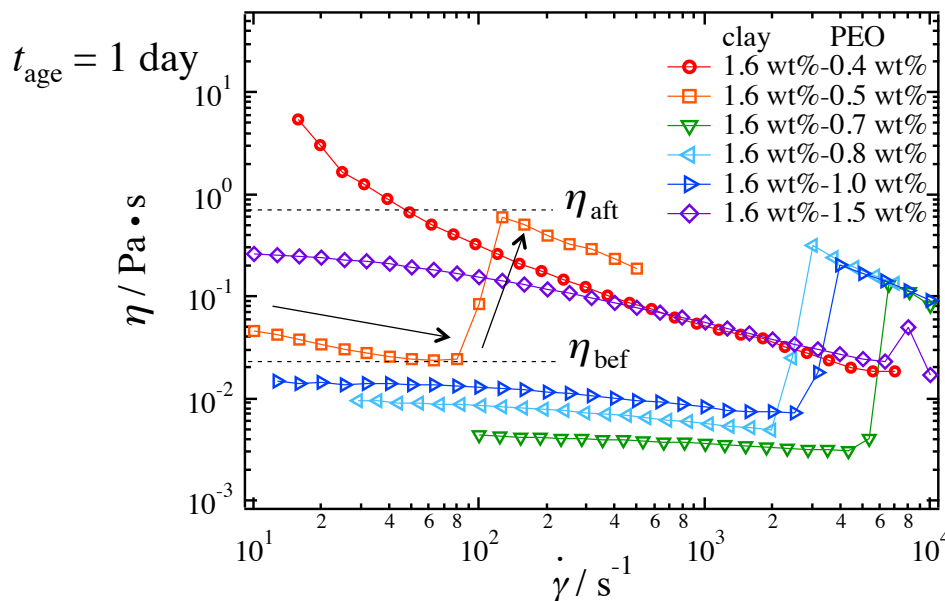


$$x \approx \gamma / N^{1/2} \approx 0.02$$

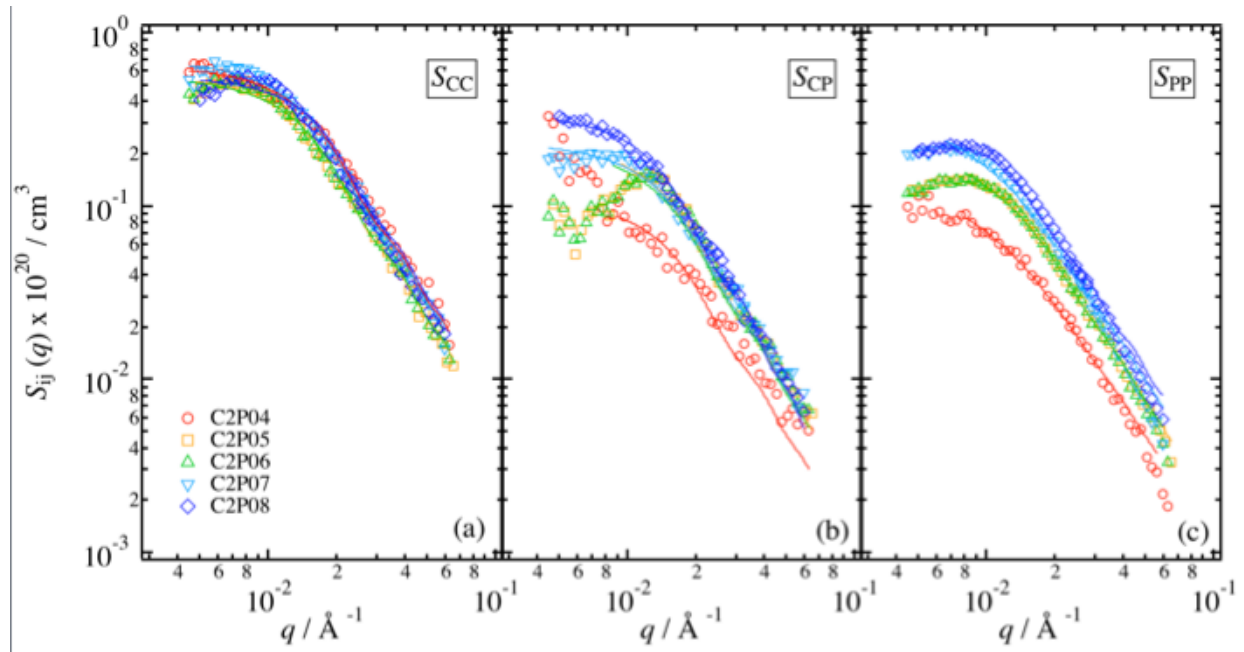
The effects of non-Gaussianity is NOT significant at all in this case.



Rheological properties of clay-PEO soln.



Shear-thickening transition took place at a finite concentration window. The strength of thickening was defined by $F = \eta_{aft} / \eta_{bef}$



67

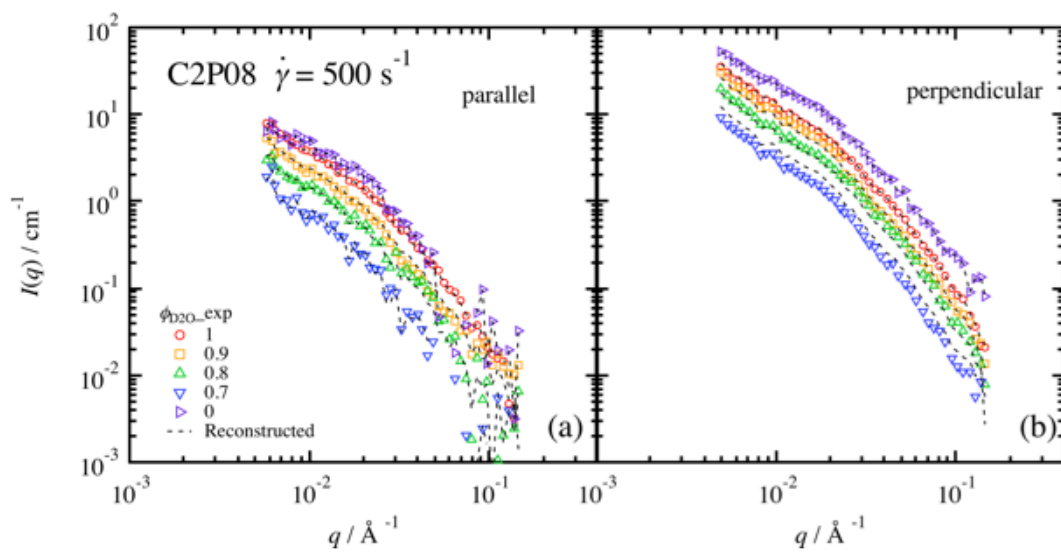


Fig.11

68

Table 2 stationary fitting parameter

	C2P04	C2P05	C2P06	C2P07	C2P08
$R_C / \text{\AA}$	150				
$D_C / \text{\AA}$	10				
ϕ_{cyl}	0.0076				
$R_{\text{pY}} / \text{\AA}$	91	72	76	76	110
prefactor	1.6	1.2	1.2	1.5	1.6
$R_{\text{pl}} / \text{\AA}$	150	150	150	150	190
$D_{\text{pl}} / \text{\AA}$	17	21	21	21	24
ϕ_{pl}	0.23	0.39	0.38	0.30	0.21
S_{pp}^0	0.082	0.12	0.14	0.19	0.25
$\xi / \text{\AA}$	110	120	120	130	180

69

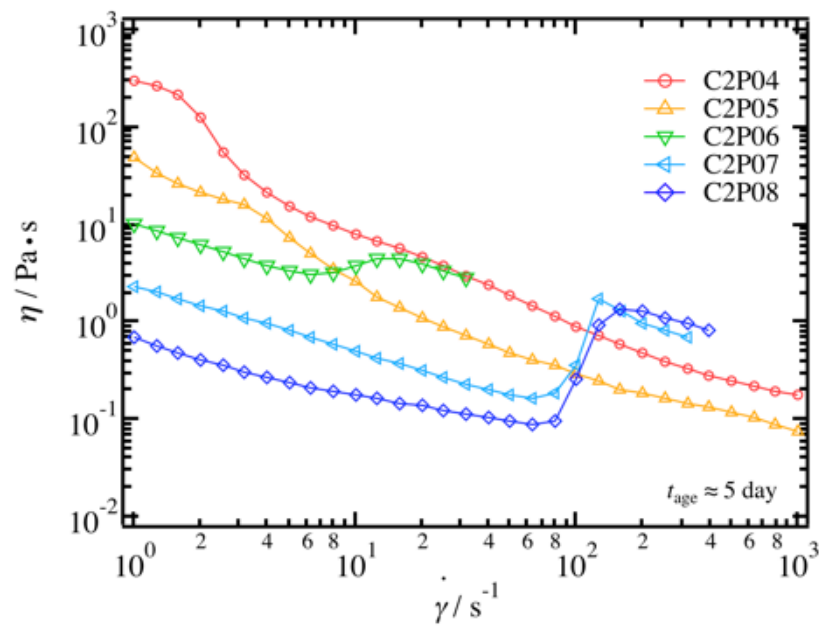


Fig.1

70

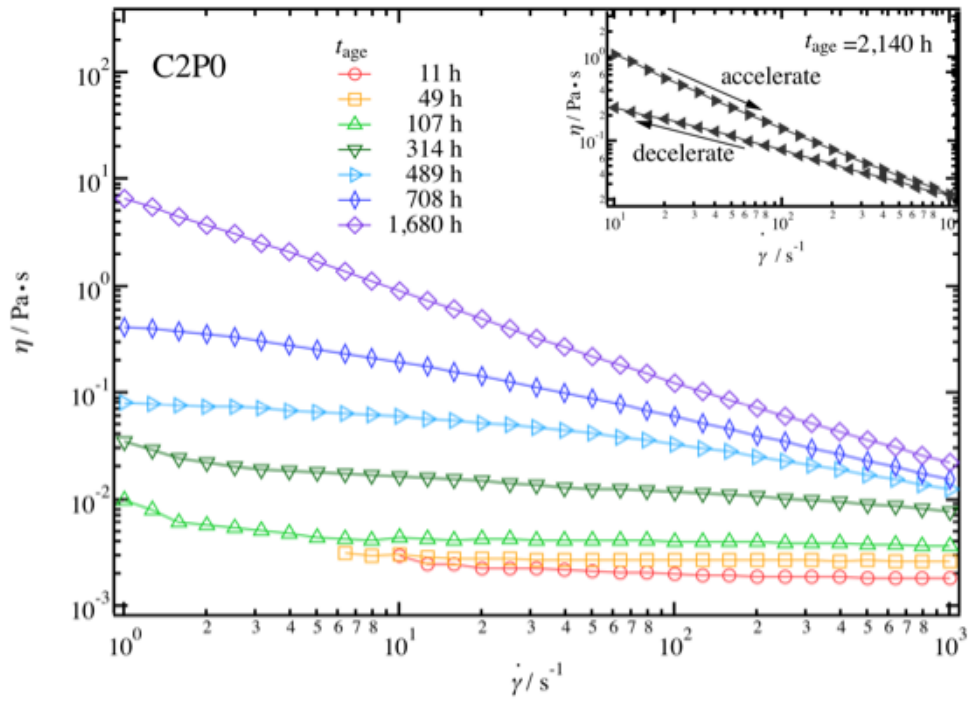


Fig.3

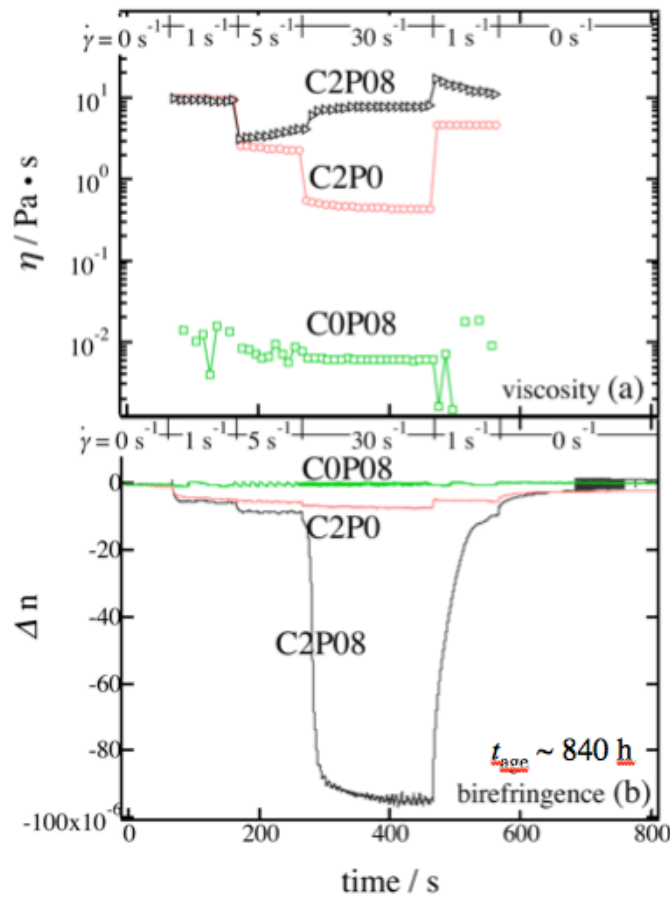
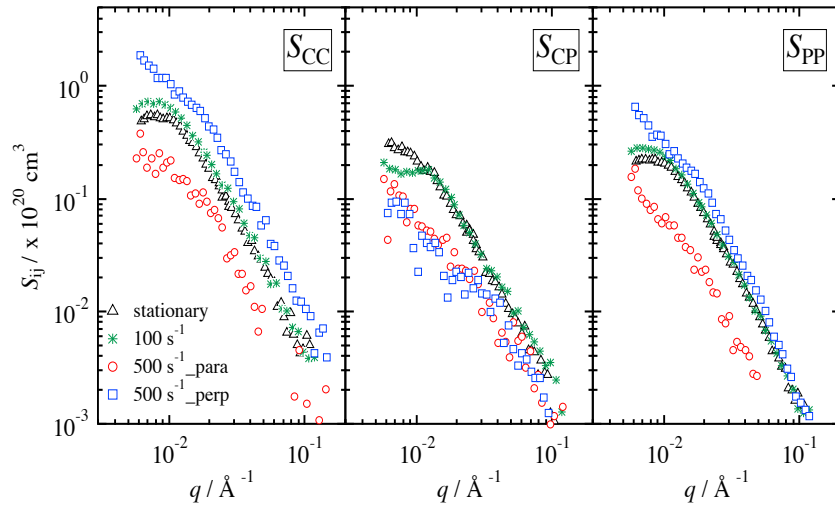


Fig.13



1D partial scattering functions (SDD = 2, 8 m)



- Partial scattering functions at 100 s⁻¹ show same patterns with 0 s⁻¹.
- There are PEO layers adsorbed on clay at each shear rate, but the layers were peeled off by shear thickening.
- Clay and PEO orient to parallel to the flow direction at 500 s⁻¹.

73

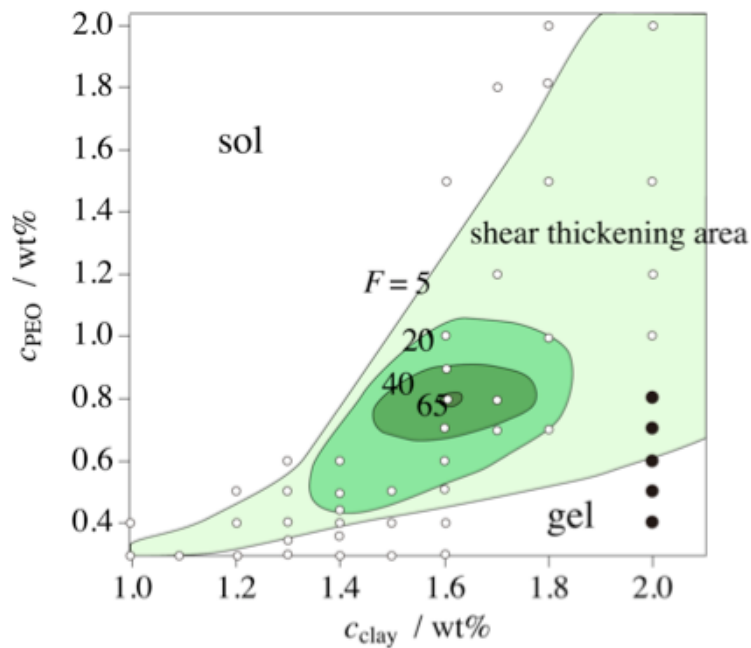


Fig.2

74

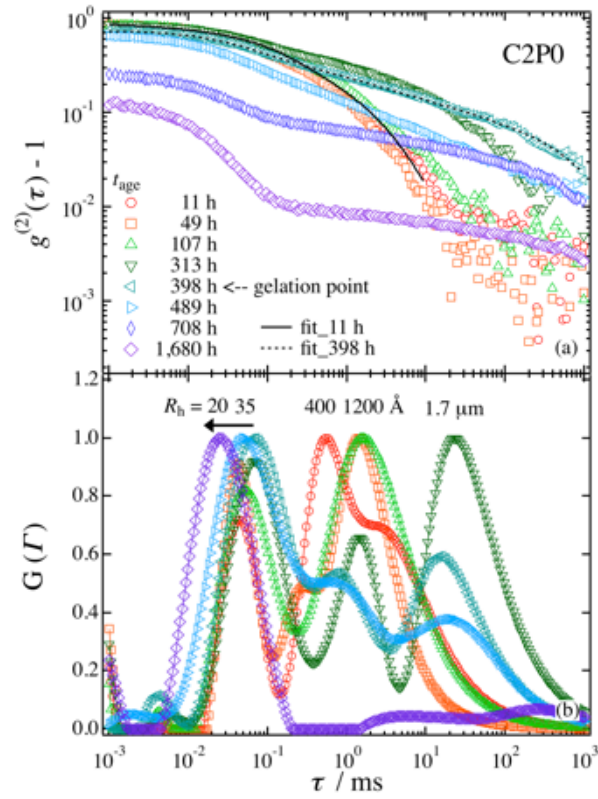


Fig.4

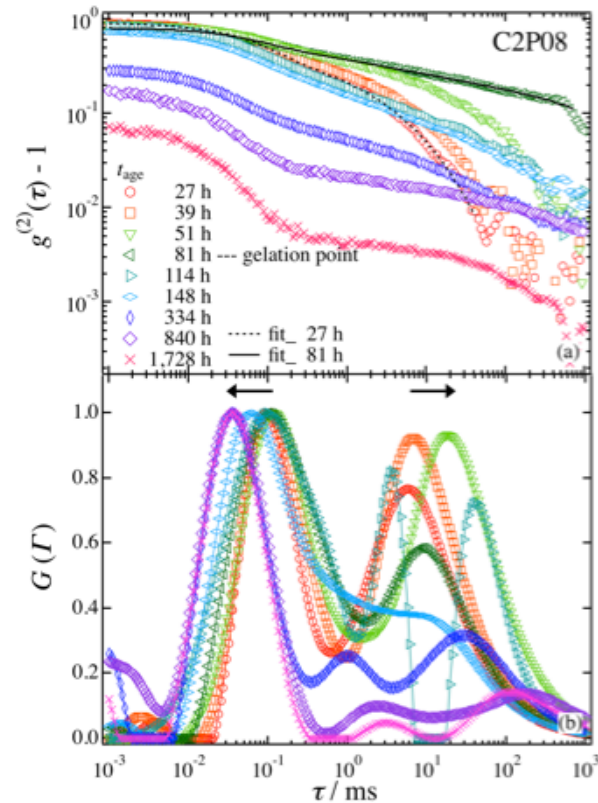


Fig.6

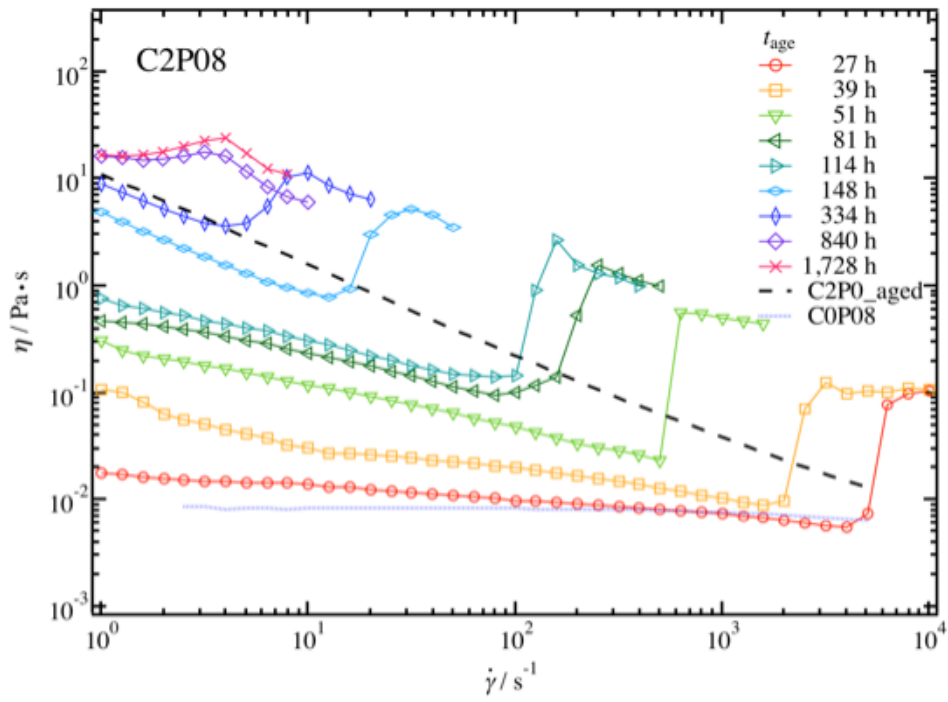


Fig.5